Published in final edited form as:
Cell Microbiol. 2010 January ; 12(1): 67–83. doi:10.1111/j.1462-5822.2009.01379.x.

Nitric oxide/cGMP Signaling Induces *Escherichia coli* K1 Receptor Expression and Modulates the Permeability in Human Brain Endothelial Cell Monolayers During Invasion

Rahul Mittal[a] and **Nemani V. Prasadarao**[a,b]

[a]Division of Infectious Diseases, The Saban Research Institute, Childrens Hospital Los Angeles, CA 90027.

[b]Keck School of Medicine, University of Southern California, Los Angeles, CA 90027.

SUMMARY

Escherichia coli K1 invasion of human bran microvascular endothelial cells (HBMEC) mediated by outer membrane protein A (OmpA) results in the leakage of HBMEC monolayers. Despite the influence of nitric oxide (NO) in endothelial cell tight junction integrity, its role in *E. coli* induced HBMEC monolayer permeability is poorly defined. Here, we demonstrate that *E. coli* invasion of HBMEC stimulates NO production by increasing the inducible nitric oxide synthase (iNOS) expression. Exposure to NO producing agents enhanced the invasion of OmpA$^+$ *E. coli* and thereby increased the permeability of HBMEC. OmpA$^+$ *E. coli*-induced NO production lead to increased generation of cGMP and triggered the expression of OmpA receptor, Ec-gp96 in HBMEC. Pre-treatment of HBMEC with iNOS inhibitors or by introducing siRNA to iNOS, but not to eNOS or cGMP inhibitors abrogated the *E. coli*-induced expression of Ec-gp96. Overexpression of the C-terminal truncated Ec-gp96 in HBMEC prevented NO production and its downstream effector, cGMP generation and consequently, the invasion of OmpA$^+$ *E. coli*. NO/cGMP production also activates PKC-α, which is previously shown to be involved in HBMEC monolayer leakage. These results indicate that NO/cGMP signaling pathway plays a novel role in OmpA$^+$ *E. coli* invasion of HBMEC by enhancing the surface expression of Ec-gp96.

Keywords

Disease processes; Mechanism of action; Microbial-cell interaction; Virulence; Infection

INTRODUCTION

Escherichia coli K1 is the most common gram-negative bacterium that causes meningitis during neonatal period. Fifty years after the advent of antibiotics, the morbidity and mortality rates associated with *E. coli* K1 (*E. coli*) meningitis remains high (Polin and Harris, 2001; Kim, 2003). An improved understanding of the pathophysiology of this disease is crucial in the endeavor to develop new preventive strategies. Among the central nervous system complications that contribute to the poor clinical outcome during an acute phase of the disease are brain edema, hydrocephalus and elevations of intracranial pressure (Tunkel and Scheld, 1993; Leib and Tauber, 1999). A high degree of bacteremia is a pre-requisite for breaching of the blood-brain barrier (BBB) in human and animal models, which is a hallmark of this disease

Address for correspondence: Nemani V. Prasadarao, Ph. D., Division of Infectious Diseases, MS #51, Childrens Hospital Los Angeles, 4650 Sunset Blvd., Los Angeles, CA 90027., Tel: 323-361-5465, Fax: 323-361-2867, pnemani@chla.usc.edu.

(Xie *et al.*, 2004). We and other investigators have shown that *E. coli* interacts with the brain microvascular endothelial cells (BMEC), which constitute a single cell lining of the BBB, to enter the central nervous system (Prasadarao *et al.*, 1996; Kim, 2003; Kim *et al.*, 2005; Shin *et al.*, 2005; Maruvada *et al.*, 2008). Additionally, *E. coli* interaction with Ec-gp96, a receptor on human BMEC (HBMEC), via the outer membrane protein A (OmpA) during invasion results in the leakage of HBMEC monolayers (Prasadarao, 2002; Prasadarao *et al.*, 2003). Infection with *E. coli* causes the disassembly of tight junctions between endothelial cells due to the separation of VE-cadherin (VEC) from other molecules of tight junctions (Sukumaran and Prasadarao, 2003). So far, it is unclear how the interaction of *E. coli* with Ec-gp96 transduces signals to disrupt the endothelial tight junctions.

There is increasing evidence that nitric oxide (NO) is an important modulator of cerebral vascular permeability (Jaworowicz *et al.*, 1998; Mayhan, 2000). Moreover, elevated NO production has been observed in animal models of bacterial meningitis and also in human patients with the disease (Suzuki *et al.*, 1999; Murawska-Ciałowicz *et al.*, 2000). NO is a pleiotropic mediator playing an important role in antimicrobial host defense against intracellular pathogens (Bogdan, 2001; Chakravortty and Hansel, 2003). NO is formed by the oxidative deamination of the amino acid L-arginine by nitric oxide synthases (NOS) (Burgner *et al.*, 1999). Three isoforms of this enzyme are described: neuronal NOS (nNOS or NOS1), inducible NOS (iNOS or NOS2) and endothelial NOS (eNOS or NOS3) (Nathan and Xie, 1994). nNOS and eNOS are expressed constitutively in the adult brain and regulate major physiological functions, including vascular hemostasis and neurotransmission. In contrast, iNOS or NOS2 is absent in resting cells, but the gene is rapidly expressed in response to stimuli such as lipopolysaccaride (LPS) or lipotechoic acid, bacteria and pro-inflammatory cytokines (Xie *et al.*, 1992; Hattor *et al.*, 1997; Boveri *et al.*, 2006). Once induced, iNOS synthesizes 100–1000 times more NO than the constitutive enzymes and does so for prolonged periods. Enhanced levels of iNOS were found at the sites of infection in animal models such as Salmonellosis, leishmaniasis, and human tuberculosis (Stenger *et al.*, 1996; Chan *et al.*, 2001; Khan *et al.*, 2001; Lahiri *et al.*, 2008). The use of knockout mice and NOS inhibitors provided evidence that NO is a major factor controlling the fate of pathogens by directly inhibiting the growth of various microbes *in vitro*. NO production has been shown to be protective in Listeric meningoencephalitis of rats (Remer *et al.*, 2001). Since NO is short-lived molecule, it triggers the formation of cGMP by NO-stimulated guanylyl cyclase and activation of cGMP-dependent protein kinase I (Cary *et al.*, 2006). It has also been shown that NO pre-conditioning produced increased association and expression of soluble guanylyl cyclase (sGC) and NOS with heat shock protein 90 (HSP90), a homologue of Ec-gp96 (Venema *et al.*, 2003; Papapetropoulos *et al.*, 2005; Antonova *et al.*, 2007). Given the importance of NO/cGMP signaling cascade in vascular permeability, we hypothesize that *E. coli* K1 interaction with HBMEC affects NO as well as cGMP responses and in turn HBMEC monolayer integrity. The present study demonstrates for the first time that infection of HBMEC with $OmpA^+$ *E. coli* elevates iNOS expression and NO production, which in turn enhances the generation of cGMP, an important downstream target of NO. Increased cGMP lead to activation of PKC-α, which is shown to be responsible for *E. coli* invasion and the permeability of HBMEC monolayers in our previous studies (Sukumaran *et al.*, 2002; Sukumaran and Prasadarao, 2002; Sukumaran *et al.*, 2003). The increased cGMP levels also enhanced the bacterial invasion due to augmented expression of Ec-gp96 in HBMEC and concomitantly increased the permeability of HBMEC monolayer.

RESULTS

Inhibitors of iNOS prevent *E. coli* induced HBMEC monolayer leakage

To examine the role of NO in *E. coli* induced HBMEC leakage, NOS inhibitors in transwell system were used to pretreat HBMEC and determined both transendothelial electrical resistance (TEER) and horseradish peroxidase (HRP) leakage. HBMEC were incubated with amino guanidine (AG, specific to iNOS), L-NAME (inhibits both iNOS and eNOS), L-NMMA, D-NMMA (inactive analog of L-NMMA) or L-arginine (control) for 1 h prior to addition of bacteria. Control uninfected HBMEC monolayers showed approximately 300–350 ohms/cm^2 TEER, which was significantly reduced to ~150 ohms/cm^2 (50–57% reduction, $P<0.001$ by Student's *t* test at each time point) after infection with OmpA$^+$ *E. coli* at a multiplicity of infection of 100 (cell and bacteria ratio, 1: 100)(Fig. 1A). Approximately 15% reduction (50–60 ohms/cm^2) in resistance was also observed with OmpA$^-$ *E. coli* infected monolayers. In agreement with these results, the permeability of the monolayers as measured by HRP leakage has also increased with OmpA$^+$ *E. coli* infection compared to OmpA$^-$ *E. coli* (9000 ± 1050 pg/ml versus 3600 ± 450 pg/ml, respectively; Fig. 1B). Of note, HBMEC monolayers pretreated with NOS inhibitors (2–4 μM concentration) maintained the resistance similar to that of control despite infection with OmpA$^+$ *E. coli*. The permeability of the monolayers induced by OmpA$^+$ *E. coli* was also substantially reduced when HBMEC were pretreated with iNOS inhibitors or included in the medium along with the bacteria in comparison to OmpA$^+$ *E. coli* infected cells ($P<0.001$ by Student's *t* test). Addition of L-arginine to HBMEC slightly enhanced both the TEER and the monolayer permeability in the presence of OmpA$^+$ *E. coli*. These results indicate that *E. coli* induced HBMEC monolayer permeability might be mediated through iNOS activation for which OmpA expression is critical. Our previous studies also demonstrated that OmpA$^+$ *E. coli* induces HBMEC monolayer permeability by disassembling the VE-cadherins at the tight junctions (TJs) (Sukumaran and Prasadarao, 2003). To examine whether iNOS inhibitors prevent this disassembly upon infection with OmpA$^+$ *E. coli*, HBMEC monolayers were infected with OmpA$^+$ or OmpA$^-$ *E. coli* in the presence or absence of iNOS inhibitors. The monolayers were fixed and stained with anti-VE-cadherin antibodies. In addition, HBMEC monolayers were also treated with a NO donor, diethylamine NONOate, to examine whether excessive production of NO induces TJ disruption. Control uninfected monolayers showed very clear boundaries of HBMEC by anti-VE-cadherin antibodies (Fig. 1C). In contrast, infection with OmpA$^+$ *E. coli* disrupted the boundary pattern in certain areas where the bacterial attachment was present. OmpA$^-$ *E. coli* infection revealed disruption of the TJs in a very few places (data not shown). Pre-treatment with AG significantly prevented the OmpA$^+$ *E. coli* induced disassembly of TJs (Fig. 1C). Of note, treatment with NONOate alone without bacterial infection also showed considerable disruption of the TJs, which is similar to HBMEC pre-treated with thrombin in our previous studies (Sukumaran and Prasadarao, 2003). Taken together these data indicate that NO is playing a major role in the *E. coli* mediated alterations of TJs of HBMEC monolayers.

E. coli K1 invasion of HBMEC is associated with the production of NO

Since NOS inhibitors prevented the HBMEC monolayer permeability, we hypothesized that the interaction of *E. coli* with HBMEC might induce the production of NO. Therefore, NO production following infection of HBMEC with OmpA$^+$ and OmpA$^-$ *E. coli* was assessed in supernatants. As predicted, OmpA$^+$ *E. coli*, which invades HBMEC efficiently induced higher levels of NO production compared to OmpA$^-$ *E. coli*, which does not invade HBMEC. The levels of NO ranged from 2.5 to 5.5 μg/ml in OmpA$^+$ *E. coli* infected cells whereas it ranged from 1 to 2.3 μg/ml in OmpA$^-$ *E. coli* ($P<0.001$ by two tailed *t* test at all time points, Fig. 2A). Peak production of NO was detectable at 60 min post-infection in both OmpA$^+$ and OmpA$^-$ *E. coli* infected cells, which was subsequently dropped to 15 min post-infection level by 90 min. The NO production in HBMEC infected with the bacteria depended on the inoculum size

with maximum levels released at an moi of 100. Pre-treating HBMEC with NOS inhibitors completely inhibited NO production despite infection with $OmpA^+$ or $OmpA^-$ *E. coli*. To investigate whether the increased production of NO by $OmpA^+$ *E. coli* is due to increased expression of iNOS and/or eNOS, Western blotting analysis of the lysates from infected HBMEC was carried out with antibodies to iNOS or eNOS. The expression of iNOS in $OmpA^+$ *E. coli* infected HBMEC was elevated at 30 min post-infection by 50% compared to the levels induced by $OmpA^-$ *E. coli* and continued to increase by two-fold at 60 min post-infection after which point it started declining (Fig. 2B). In contrast, the expression of eNOS was elevated only by 10% at 30 min, which remained constant up to 90 min post-infection. Next, total RNA was isolated from HBMEC infected with *E. coli* for varying periods and examined for the increased transcript of iNOS and eNOS by RT-PCR. Peak transcription of iNOS was observed at 60 min post-infection, whereas eNOS transcription was marginally increased in comparison to $OmpA^-$ *E. coli* induced levels (Fig. 2C). These results suggest that OmpA expression is required in *E. coli* to induce higher levels of NO production by increasing the transcription of iNOS and to some extent, of eNOS at the gene level in HBMEC, which correlates with the invasion frequency of the bacteria.

iNOS activation contributes to the invasion of HBMEC by *E. coli* K1

To further confirm the effect of NO production on the invasion of HBMEC by *E. coli*, NOS inhibitor AG was used to pretreat the cells in invasion assays. Significant reduction (>90%) in the invasion of $OmpA^+$ *E. coli* was observed following treatment with AG in comparison to untreated or L-arginine treated cells (Fig. 3A, $P<0.001$ by two tailed Student's *t* test). Addition of AG along with bacteria to HBMEC (Bacteria+AG) also showed similar inhibitory effect on the invasion. Although no statistically significant difference was observed in the total cell associated *E. coli* K1 to HBMEC after pretreatment with AG compared to untreated cells, there was a ~7% decrease in binding of the bacteria (Fig. 3B). To further confirm the role of iNOS in *E. coli* invasion of HBMEC, siRNA to iNOS or eNOS was introduced into HBMEC. The transfected cells were then examined for iNOS or eNOS mRNA transcription by RT-PCR. Complete suppression of iNOS transcription despite infection with $OmpA^+$ *E. coli* in iNOS-siRNA/HBMEC was observed, whereas iNOS transcription in eNOS-siRNA/HBMEC was not affected (Fig. 4A). Similarly, the mRNA levels of eNOS were completely absent in eNOS-siRNA/HBMEC but not iNOS mRNA levels (data not shown). Basal level production of NO in iNOS-siRNA/HBMEC were observed when infected with $OmpA^+$ *E. coli* for various time points, whereas eNOS-siRNA/HBMEC showed normal production (Fig. 4B). Similarly, NONOate-induced production of NO by HBMEC was also completely abrogated in iNOS-siRNA/HBMEC. Transfection with eNOS-siRNA had no effect on the production of NO with any of the treatments. Flow cytometry analysis revealed that iNOS expression was completely abolished in iNOS-siRNA/HBMEC despite infection with either $OmpA^+$ or $OmpA^-$ *E. coli* compared to control siRNA infected HBMEC (Fig. 4C). In contrast, eNOS-siRNA/HBMEC revealed iNOS expression similar to that of control cells. Furthermore, the siRNA transfected HBMEC treated with NONOate showed an increase in iNOS expression in control siRNA/HBMEC similar to that of non-transfected HBMEC. However, the increased expression of iNOS was completely abrogated in iNOS-siRNA/HBMEC. In addition, very little invasion (<10%) of *E. coli* into iNOS-siRNA/HBMEC, but not eNOS-siRNA/HBMEC transfected cells was observed, suggesting that iNOS plays a major role in the invasion process (Fig. 4D). The binding of $OmpA^+$ *E. coli* to iNOS-siRNA/HBMEC was also reduced by 25% compared to control siRNA transfected HBMEC. The binding of $OmpA^+$ *E. coli* to AG pre-treated/- and iNOS-siRNA/HBMEC differed slightly because AG pre-treatment would not block the constitutive expression of Ec-gp96 whereas iNOS-siRNA transfection did block the receptor expression. No decrease in binding of the bacteria to eNOS-siRNA/HBMEC was noted, indicating that iNOS activation is important for increased invasion of $OmpA^+$ *E. coli*.

Enhanced production of NO modulates the invasive ability of *E. coli* by controlling the expression of Ec-gp96 in HBMEC

We speculated that if NO is involved in the invasion process, then increase in NO production might augment the ability of *E. coli* to invade HBMEC. To examine this, we treated HBMEC with histamine (1 μM) or NONOate (5 μM) and invasion assays were performed. Interestingly, increased NO production by HBMEC by NO inducers not only increased the binding (total cell associated bacteria) but also the invasive ability of *E. coli* (Fig. 5A and 5B). The number of intracellular bacteria in NONOate treated HBMEC was significantly higher compared to untreated cells ($1.1 \times 10^5 \pm 0.7 \times 10^5$ cfu/well vs. $4 \times 10^4 \pm 0.55 \times 10^4$ cfu/well respectively, $P<0.001$ by Student's *t* test). A similar increase in the invasion was also observed in histamine treated HBMEC. Of note, the binding of *E. coli* to histamine or NONOate treated HBMEC was increased by 50% compared to untreated HBMEC (Fig. 5A). Neither binding nor invasion of OmpA$^-$ *E. coli* was affected by these treatments. Furthermore, invasion of another meningitis causing bacterium, Group B streptococcus (GBS), was used to verify whether the increase in invasion is specific to *E. coli*. GBS invade HBMEC with a similar frequency to that of *E. coli* in HBMEC (Maruvada *et al.*, 2008b). Neither the binding nor the invasion of GBS was increased in histamine or NONOate treated HBMEC (Fig. 5C). These results suggest that increased NO production helps *E. coli* in enhanced binding to and invasion of HBMEC.

Our studies have shown that *E. coli* interacts with Ec-gp96 via OmpA to invade HBMEC (Prasadarao, 2002). Therefore, to evaluate whether Ecgp-96 expression is critical for the production of NO in HBMEC, siRNA to Ec-gp96 was introduced into the cells. The expression of Ec-gp96 after siRNA transfection was verified by flow cytometry and these data revealed that >95% of the surface expression was reduced on HBMEC in comparison to the cells transfected with control siRNA (data not shown). The cells were then infected with OmpA$^+$ or OmpA$^-$ *E. coli*, or treated with NONOate and the production of NO was determined. More than 90% reduction in NO levels was observed in Ec-gp96-siRNA/HBMEC infected with OmpA$^+$ *E. coli* infected cells, whereas 10% reduction was observed in OmpA$^-$ *E. coli* infected cells in comparison to control-siRNA/HBMEC (Fig. 6A). In contrast, NONOate induced similar levels of NO in either Ec-gp96-siRNA/HBMEC or control-siRNA/HBMEC. Nonetheless, the lack of NO production in Ecgp-96-siRNA/HBMEC infected with OmpA$^+$ *E. coli* is due to a very negligible invasion (Fig. 6B). The binding of OmpA$^+$ *E. coli* to Ec-gp96-siRNA/HBMEC was also reduced by 15%. Neither the binding nor the invasion of GBS into these cells was affected, suggesting that *E. coli* interaction with Ecgp-96 mediated by OmpA is critical for the enhanced production of NO by HBMEC. Next, to examine whether NO production by *E. coli* in HBMEC affects Ec-gp96 expression, HBMEC infected with OmpA$^+$ and OmpA$^-$ *E. coli*, histamine or NONOate were stained with anti-Ec-gp96 antibodies and subjected to flow cytometry. Only a certain population of uninfected HBMEC showed positive Ec-gp96 expression in agreement to our previous studies (Prasadarao, 2002), whichh was increased by two-fold after infection with OmpA$^+$ *E. coli* (Fig. 6C). In contrast, OmpA$^-$ *E. coli* infection induced a 5–10% increase in the expression of Ec-gp96 in comparison to control cells. HBMEC treated with AG and infected with OmpA$^+$ *E. coli* showed a significant reduction in the expression of Ec-gp96, which was below the basal levels compared to OmpA$^+$ *E. coli* infected cells. HBMEC transfected with siRNA to iNOS, but not eNOS also showed below the basal level expression of OmpA receptor. A substantial increase (>4-fold) in the expression of Ec-gp96 was observed in HBMEC treated with both histamine and NONOate. The increased Ec-gp96 expression depends on dose-dependent treatment with the NO inducers (data not shown). In contrast, GBS invasion of HBMEC induced the expression of Ec-gp96 by only 10%, suggesting that the phenomenon of receptor expression upon NO production in HBMEC is specific to *E. coli* invasion. Taken together, these results suggest that Ec-gp96 expressed constitutively on the surface of HBMEC might have been endocytosed

during the initial batch of *E. coli* invaded and subsequent induction of Ec-gp96 expression is responsible for additional bacterial entry.

Overexpression of truncated Ec-gp96 prevents the iNOS activation by *E. coli*

To examine whether the interaction of OmpA$^+$ *E. coli* with Ec-gp96 transduces signals to activate iNOS expression, two C-terminal truncated Ec-gp96 constructs were overexpressed in HBMEC and examined the production of NO. In addition, full-length (FL) Ec-gp96 was also expressed in HBMEC as a positive control. Only ~25% of plasmid alone transfected cells showed the expression of Ec-gp96 on its surface, which was doubled in all the three HBMEC transfectants (Fig. 7A). CD44 expression, used to verify whether the transfection with the plasmid alters the surface expression of other markers in HBMEC, demonstrated no differences between the transfectants. The expression of the truncated proteins was also examined by Western blotting with anti-Ec-gp96 antibody. Fig. 7B revealed that control cells expressed 96 kDa and 65 kDa proteins, whereas Ec-gp96Δ400 showed a minor 96 kDa and a major 50 kDa protein. Total cell lysates from Ec-gp96Δ200 exhibited an approximately 60 kDa protein, while FL-Ec-gp96 revealed 96 and 65 kDa proteins. The protein band pattern observed with control and FL-Ec-gp96 lysates is in agreement with our previous studies in which HBMEC lysates exhibit a 96 kDa and a 65 kDa cleavage product. Truncation of C-terminal 200 and 400 amino acids resulted in 65 and 50 kDa proteins, respectively. These results suggest that the full length and truncated Ec-gp96 proteins are expressed in good quantities on the surface of HBMEC. Furthermore, the binding of OmpA$^+$ *E. coli* to both Ec-gp96Δ200 and Ec-gp96Δ400 transfected HBMEC was similar to that of FL-Ec-gp96/HBMEC, which is 25–35% higher than the binding to control cells. However, a significant decrease in the invasion was observed in Ec-gp96Δ200/- and Ec-gp96 Δ400/HBMEC while a 60% increase in the invasion with FL-Ec-gp96/HBMEC was detected (Fig. 7C). Decreased production of NO in Ec-gp96Δ200/- and Ec-gp96Δ400/HBMEC following interaction with *E. coli* was observed, which was correlated with the decrease in invasion (Fig. 8A). FL-Ec-gp96/HBMEC produced 50% higher levels of NO when infected with OmpA$^+$ *E. coli* compared to plasmid alone-transfected cells (pHBMEC). The monolayers formed by Ec-gp96Δ200 and Ec-gp96Δ400 transfected HBMEC also demonstrated resistance to *E. coli* induced permeability as measured by TEER and HRP leakage (Fig. 8B and C). In contrast, FL-Ec-gp96/HBMEC showed greater drop in TEER and increase in leakage of HRP compared to plasmid alone transfected HBMEC. These results suggest that the C-terminal portion of Ec-gp96 is important for transducing signals for the invasion of OmpA$^+$ *E. coli* and for the production of NO in HBMEC.

Induction of iNOS expression is associated with increased cGMP levels in HBMEC upon infection with OmpA$^+$ *E. coli*

NO is a soluble gas that can diffuse through the cell membrane. It activates the enzyme guanylyl cyclase in the cytoplasm to produce cGMP, which in turn can regulate cGMP-dependent protein kinase I (Krumenacker and Murad, 2006; Denninger, and Marlet, 1999). Therefore, the production of cGMP was determined in HBMEC lysates, infected with either OmpA$^+$ or OmpA$^-$ *E. coli*. OmpA$^+$ *E. coli* infected cells showed a significant increase in cGMP levels compared to OmpA$^-$ *E. coli* infected cells, which showed a marginal increase (Fig. 9A). The elevation in cGMP levels was completely abrogated in HBMEC pretreated with AG upon infection with OmpA$^+$ *E. coli* highlighting the importance of NO/cGMP signaling. Therefore, the effects of cGMP inhibitors or activators on HBMEC monolayer permeability were also determined. ODQ that inhibits guanylyl cyclase (Golombek *et al.*, 2004; Pearce *et al.*, 2009) and 8-Br-cGMP, a membrane permeable analog of cGMP (Petrov *et al.*, 2008; Murphy *et al.*, 2009) were used to pre-treat HBMEC prior to infection with the bacteria. No cytotoxicity of these compounds on HBMEC was observed as determined by MTT cytotoxicity assay (data not shown). ODQ significantly inhibited the production of cGMP by itself and even after infection with OmpA$^+$ *E. coli*, whereas the Br-cGMP showed a further increase (Fig. 9A).

Similarly, the TEER of HBMEC monolayers was greater than the control cells after treatment with ODQ, whereas significantly lower in 8-Br-cGMP treated cells in comparison to control uninfected cells (Fig. 9B). These data demonstrate that cGMP is the downstream effector molecule for NO to induce alterations in HBMEC monolayers. The expression of Ec-gp96 was significantly inhibited in ODQ pretreated and OmpA$^+$ *E. coli* infected HBMEC, whereas pretreatment with 8-Br-cGMP induces a four-fold increase (Fig. 9C). In agreement with the expression of Ec-gp96, the invasion of OmpA$^+$ *E. coli* was significantly prevented by ODQ pretreatment compared to control HBMEC (Fig. 9D). Pretreatment of HBMEC with 8-Br-cGMP again increased the invasion by 3-fold. The total cell associated bacteria in ODQ treated cells was not changed, whereas 8-Br-cGMP treatment increased the binding of the bacteria to HBMEC by 50% (Fig. 9D). Taken together, these data suggest that *E. coli* infection of HBMEC induces NO, which in turn activates cGMP signaling that causes the upregulation of Ec-gp96 for the invasion of OmpA$^+$ *E. coli* in HBMEC.

Activation of PKC-α by cGMP during OmpA$^+$ *E. coli* invasion of HBMEC

Our previous studies have shown that PKC-α activation is required for the disassembly of VEC in endothelial cells, which results in the leakage of HBMEC monolayer (Sukumaran and Prasadarao, 2003). In addition, the activation of PKC-α has been shown to be mediated by cGMP-dependent protein kinase I (Hou *et al.*, 2003). Therefore, activation of PKC-α by cGMP inducers or inhibitors in HBMEC with or without *E. coli* K1 infection was examined using PepTag non-radioactive assay (Sukumaran *et al.*, 2002; Sukumaran and Prasadarao, 2002). OmpA$^+$ *E. coli* induced the activation of PKC-α between 15 and 30 min post infection, which was completely abrogated by pretreating the cells with AG (Fig. 10A). In contrast, OmpA$^-$ *E. coli* did not show such activation in HBMEC (data not shown). NONOate by itself induced activation of PKC-α, which was further increased with OmpA$^+$ *E. coli* infection of HBMEC. Quantitative estimation of the phosophorylated peptides revealed that the activation of PKC-α was ten times higher in NONOate treated and *E. coli* infected cells at 60 min post-infection in comparison to bacteria infected cells only (Fig. 10B). Similarly, 8-Br-cGMP also induced the activation of PKC-α by itself (similar to NONOate treated-panel) and in the presence of OmpA$^+$ *E. coli* (Fig. 10A). In contrast, ODQ pretreatment of HBMEC completely abrogated *E. coli* induced activation of PKC-α activation. To further confirm the role of PKC-α, HBMEC transfected with a dominant negative form of PKC-α, PKC/CAT/KR (Sukumaran, *et al.*, 2003), were also treated with NONOate. In contrast to plasmid alone transfected HBMEC, the PKC/CAT/KR-HBMEC either with or without pre-treatment with NONOate showed no phosphorylation of PKC-α despite infection with OmpA$^+$ *E. coli* (Fig. 10C). The PKC/CAT/KR-HBMEC despite pre-treated with NONOate and infected with OmpA+ *E. coli* showed no decrease in TEER also (data not shown). Considering our previous results in which PKC/CAT/KR-HBMEC were resistant to *E. coli* induced TEER decrease, these data suggest that NO/cGMP production due to *E. coli* interaction with HBMEC mediated by OmpA induces PKC-α activation. The activated PKC-α subsequently signals for both *E. coli* invasion and HBMEC permeability.

DISCUSSION

The blood-brain barrier (BBB) plays an important role in maintaining the cerebral fluid composition and the environment of the nerve cells (Engelhardt, 2003; Zlokovic, 2008). Alterations in cerebrovascular permeability promote serious pathophysiologic disturbances, which subsequently progress to vasogenic cerebral edema, intracranial hypertension and neuronal dysfunction (Boje, 1996). NO has been reported to be an important mediator and plays a crucial role in modulating the acute pathophysiological process and brain injury associated with bacterial meningitis (Leib and Tauber, 1999). Very high levels of NO in the CSF have been observed in patients with meningitis and appear to correlate with a high

incidence of fatal outcomes (Bratasz *et al*., 2004). Although, the interaction of *E. coli* K1 with HBMEC is associated with increased permeability of HBMEC monolayer (Sukumaran and Prasadarao, 2003), the effect of bacterial invasion on NO is unexplored.

One of the novel findings of this study is that OmpA expressing *E. coli* induces significantly greater production of NO by triggering iNOS expression. Although the binding of $OmpA^-$ *E. coli* and $OmpA^+$ *E. coli* to HBMEC was not substantially different, $OmpA^-$ *E. coli* failed to produce similar amounts of NO. An important point to note here is that $OmpA^+$ *E. coli* invades HBMEC at a frequency of ~1% (one bacterium per 100 cells) whereas $OmpA^-$ *E. coli* does not invade the cells. In agreement with the invasion frequency of $OmpA^+$ *E. coli*, we have demonstrated that the OmpA receptor express only on 10–15% population of HBMEC (Prasadarao *et al.*, 1996). Therefore, *E. coli* adherence to HBMEC is mediated by both OmpA and other molecules, of which OmpA-mediated adherence is responsible for the invasion of *E. coli*. Thus, low-level production of NO by $OmpA^-$ *E. coli* could be due to the interaction of LPS with TLRs. Our previous studies have shown that both the interaction of $OmpA^+$ and $OmpA^-$ *E. coli* with HBMEC stimulates similar quantities of TNF-α and other cytokines (Selvaraj *et al.*, 2007). Therefore, the role of cytokines in the production of NO might be similar with these two strains of bacteria. Several studies have shown that cytokines require long periods (>4 h) to induce any permeability changes in endothelial cells. This contrasts with our studies in which the permeability changes were occurred within 60 min post-infection. Here, we have not explored the use of purified OmpA to examine its effect on the production of NO as it looses the three-dimensional structure required to interact with its receptor, Ec-gp96. Nonetheless, our previous studies have demonstrated that the anti-OmpA antibodies prevent the invasion of *E. coli* K1 in HBMEC and subsequent permeability changes. In agreement with the role of NO in the BBB leakage, NOS inhibitors significantly prevented the *E. coli* induced permeability changes in HBMEC monolayer, an *in vitro* model of the BBB. The profound enhancement of HBMEC permeability by NO inducers, NONOate and histamine further substantiate the role of NO. Two other studies, however, showed that TEER of HBMEC monolayer increases or permeability decreases with NONOate treatment, which results are in contrast to the data presented here (Wong *et al.*, 2004; Winter *et al.*, 2008). This discrepancy could be due to the use of 10 times lower concentrations of NONOate in our study in comparison with other studies.

Similar production of NO by infected endothelial cells also contributed to the changes in vascular permeability that occurs during acute rickettsioses (Woods and Olano, 2008). It was determined that the addition of the NO donor, DETA NONOate at certain levels results in a dose-dependent change in electrical resistance across the monolayer while effectively limiting the number of intracellular rickettsiae in human microvascular endothelial cells. In contrast, treatment with NONOate and histamine enhanced the invasion of *E. coli* in HBMEC. *Neisseria meningitidis* also induces robust production of NO in mouse derived cerebrovascular endothelium, which resulted in the loss of cell viability (Constantin *et al.*, 2004). Thus, NO produced by diverse bacteria in endothelial cells affect the outcome differently. Although NO and RNI might have direct antibacterial effects on intracellular pathogens, *E. coli* K1 utilizes the NO production to invade HBMEC. *N. meningitidis* prevents macrophage apoptosis via genes encoding nitric oxide detoxification and a porin, PorB (Tunbridge *et al.*, 2006). Contrary to this, the interplay of pneumococcal hydrogen peroxide and host derived NO play a major role in cellular damage in meningitis by *S. pneumoniae* (Hoffmann *et al.*, 2006). However, it is still to be determined whether *E. coli* K1 possesses any NO detoxification mechanisms to survive in HBMEC.

Another compelling finding of this study is that the *E. coli*-induced iNOS activation enhances the surface expression of Ec-gp96 in HBMEC. A threshold level of NO production might be necessary for driving Ec-gp96 to the cell surface and therefore, its expression was not

demonstrable in HBMEC infected with OmpA^{-} *E. coli* in which NO levels are below the threshold amounts. However, OmpA mediated interaction of *E. coli* with Ec-gp96 induces two fold higher levels of NO, which is responsible for enhanced expression of OmpA receptor. NO transduces most of its biological effects through the activation of heterodimeric enzyme, soluble guanynyl cyclase (sGC). Activation of sGC results in the production of cGMP from GTP, which is then involved in the activation of a variety of effectors such as cyclic nucleotide gated channels, protein kinases, and phosphodiesterases (Poulos, 2006; Derbyshire and Marletta, 2009). This NO/cGMP signaling pathway is important in mediating numerous physiological processes including vascular and non-vascular smooth muscle relaxation, platelet reactivity, phototransduction and peripheral and central neurotransmission (Denninger and Marletta, 1999; Krumenacker and Murad, 2006). In this study, we observed that *E. coli* K1 induces the production of NO, which then triggers the synthesis of cGMP that in turn enhances the expression of Ec-gp96. Of note, cGMP production also activated PKC-α, which in turn is responsible for HBMEC monolayer permeability as demonstrated earlier (Sukumaran and Prasadarao, 2003). The activated PKC-α was shown to cause disassembly of the tight junctions near *E. coli* attachment site but not away from the bacterial binding location. Of note, *N. meningitidis* adhesion to human brain endothelial cells was found to recruit a polarity complex containing Par3/Par6/PKCζ, which eventually responsible for opening of the intracellular junctions (Coureuil et al, 2009). Therefore, further studies are needed to examine whether similar polarity complex containing PKC-α and other junctional molecules would be responsible for the HBMEC monolayer leakage induced by *E. coli*.

Other investigators have reported that sGC interacts with HSP-90, a homologue of Ec-gp96, and eNOS/iNOS (Venema *et al.*, 2003; Papapetropoulos *et al.*, 2005; Antonova *et al.*, 2007). It is interesting that the distribution of sGC between membrane and cytosolic fraction differs with cell type: 80% of sGC in endothelial cells is membrane-associated, and only 20% is in a freely soluble cytosolic form. Therefore, HSP90/sGc/NOS complexes would facilitate the autocrine actions of NO by bringing together the NO source and its target; the proximity of NOS with sGC could preserve critical NO functions during oxidative stress (Antonova *et al.*, 2007). Of note, Yoshida and Xia identified HSP90 as an important endogenous protein enhancer of iNOS (Yoshida and Xia, 2003). Therefore, increased expression of iNOS and its localization to the cell surface might drive Ec-gp96 to insert in the plasma membrane either independently or as a complex with iNOS/sGC in HBMEC (Fig. 11). The expression of gp96 in the host is considered to be a danger signal to recruit PMNs to sites of infection (Panjwani *et al.*, 2002). Nonetheless, *E. coli* K1 takes advantage of Ec-gp96 expression not only to invade HBMEC but also to mask the danger signal on the cell. Similar to these studies exogenous NO directly activated the expression of glucocorticoid receptor, although higher concentrations of NONOate were used in these experiments (Ji and Diamond, 2004). It is still to be determined whether *E. coli* induced iNOS interacts with Ec-gp96 during the recruitment to cell surface. The newly expressed Ec-gp96 would function as additional receptors to OmpA^{+} *E. coli* for an enhanced invasion. Since truncated Ec-gp96 expressing HBMEC did not show increased NO production, we assume that the C-terminal domain of Ec-gp96 is necessary for intracellular signaling to induce *E. coli* internalization.

In summary, the present study demonstrates a novel phenomenon that *E. coli* interaction with HBMEC induces NO production by enhancing the iNOS expression for which initial interaction of OmpA with its receptor Ec-gp96 is necessary. The invasion of *E. coli* in HBMEC also triggered the further cell surface expression of Ec-gp96 and activated PKC-α via cGMP production, which has been shown to be important for both invasion and the disassembly of tight junctions of HBMEC in our previous studies. Therefore, strategies to inhibit the OmpA-Ec-gp96 interaction would be helpful to develop new treatment options for preventing *E. coli* K1 meningitis in neonates.

EXPERIMENTAL PROCEDURES

Bacterial strains, antibodies and other reagents

E. coli E44 ($OmpA^+$ *E. coli*) is a rifampin-resistant mutant of *E. coli* K1 strain RS 218 (serotype O18:K1:H7), which was isolated from the cerebrospinal fluid of a neonate with meningitis, and invades human brain microvascular endothelial cells *in vitro* (Prasadarao *et al.*, 1996). $OmpA^-$ *E. coli* is a noninvasive derivative of E44 that expresses no OmpA, since the ompA gene is disrupted (Prasadarao et al, 1996). GBS Type III strain COH-1 (GBS) is a tetracycline resistant clinical isolate from an infected patient and is highly encapsulated (Maruvada *et al.*, 2008b). Bacteria were grown in brain heart infusion broth (Difco Laboratories) with appropriate antibiotics. Antibodies to iNOS, eNOS and β actin were obtained from BD Biosciences (San Diego, CA) and Santa Cruz Biotechnology (San Diego, CA), respectively. Anti-Ec-gp96 antibody was generated in our lab and described previously (Prasadarao, 2002; Prasadarao *et al.*, 2003). Horseradish peroxidase, L-NAME, L-NMMA, D-NMMA, amino guanidine, histamine, NADPH, nitrate reductase, Griess reagent and diethyl amine NONOate were obtained from Sigma (St. Louis, MO). ODQ and Br-cGMP were obtained from Calbiochem (San Diego, CA). VE-cadherin antibody was obtained from Cell Signaling Technology Inc. (Danvers, MA).

Cell culture and invasion assays

Human brain capillaries were isolated from small fragments of cerebral cortex, which were obtained from surgical resections of 4- to 7-year-old children with seizure disorders at Children's Hospital Los Angeles. Microvascular endothelial cells (HBMEC) were isolated from these capillaries and cultured as described previously (Stins *et al.*, 1994). HBMEC were maintained at 37 °C in a humidified atmosphere of 5% CO_2 in medium containing M-199/Ham F-12 (1:1 vol/vol) supplemented with 10% fetal bovine serum, sodium pyruvate and 2 mM glutamine and cultivated in a cell culture incubator at 5% CO_2 and 37 °C. HBMEC were used between 12 and 16 passages for all the experiments. For invasion assays, HBMEC grown in 24-well cell culture plates to 95% confluence were infected with 10^7 cfu of *E. coli* strains in experimental medium (1:1 mixture of Ham F-12 and M-199 containing 5% heat inactivated fetal bovine serum) and incubated for 90 min at 37°C in an atmosphere containing 5% CO_2. The monolayers were washed three times with RPMI 1640 medium followed by addition of gentamicin (100 μg/ml) and further incubated for 1 h at 37 °C. Then the cells were washed three times with RPMI 1640 and lysed with 0.5% of Triton X-100. The released bacteria were diluted with saline and enumerated by plating on blood agar. The total cell associated bacteria were determined as described for invasion, except that the gentamicin step was omitted. To study the effect of L-NAME, aminoguanidine (AG), L-NMMA, or D-NMMA, HBMEC were treated with these inhibitors (2–4 μM) at 37°C for 1 h, followed by infection with *E. coli*. The concentrations of inhibitors were selected based on the preliminary experiments for optimal inhibition or activation. In some experiments, these substances were added along with the bacteria to HBMEC and then invasion or total binding was assessed. Results were expressed as an average of bacterial colony forming units (CFU) recovered per well from five independent determinations ± S.D. of the mean. The effect of these inhibitors on the growth of *E. coli* or GBS was assessed by culturing the bacteria in the presence of the inhibitors for varying periods and plating the aliquots of culture on agar containing appropriate antibiotics.

Generation of truncated Ec-gp96 constructs

To amplify the full length *Ec-gp96* gene (FL-Ec-gp96) coding for 803 amino acids, RT-PCR was performed on total mRNA from HBMEC using the following primer set – FP, 5' TAAGAATTCCGCCATGAGGGCCCTGTG 3' and RP, 5' CCTCTAGACTACTTGTCGTCATCGTCTTTGTAGTCTTCAGCTGTAGATT 3'. Ec-gp96Δ200, a mutant of FL-Ecgp that is devoid of 214 amino acids from the C-terminal was

amplified using the FP for FL-Ec-gp96 and the RP, 5' CCTCTAGACTACTTGTCGTCATCGTCTTTGTAGTCCTGGAACCTCTTC 3'. A RP 5'-CCTCTAGACTACTTGTCGTCATCGTCTTTGTAGTCTCTGGAACCTCTTC-3' was used to generate Ec-gp96Δ400. Both constructs contained a FLAG epitope at the C-terminal end. The amplified products were cloned into the restriction sites *Eco*RI and *Xba*I of pcDNA3.1. The resulting plasmids were transformed into DH5-α and the purified plasmids subjected to DNA sequencing to verify sequence integrity. For stable transfection, HBMEC were transfected with either Ec-gp96 mutants or empty vector using Lipofectamine reagent (Invitrogen, Carlsbad, CA), allowed to recover for 24 h, and the transfected cells were selected using 300 μg/ml of G418.

Western blotting

Confluent cell cultures in 100 mm dishes were incubated with either $OmpA^+$ or $OmpA^-$ *E. coli* for varying time points at 37°C. The cells were then rinsed with ice-cold phosphate buffered saline (PBS) and scraped off into 500 μl of RIPA buffer (1 × PBS, 1% Nonidet P-40, 0.5% sodium deoxycholate, 0.1% SDS, 10 μg/ml PMSF, aprotinin, and 1 mM sodium orthovanadate). Cells were mildly sonicated and the lysates were clarified by centrifugation for 10 min at 10, 000 × *g* to remove cell debris. The supernatants were collected and protein concentrations were determined by using a Bio-Rad protein assay. Approximately 30 μg of total protein was subjected to polyacrylamide gel electrophoresis on 10 % SDS polyacrylamide gel by using a Bio-Rad Mini PROTEAN II apparatus. Proteins were then transferred to nitrocellulose membranes using a Bio-Rad semi-dry transfer apparatus. The blot was incubated with blocking buffer (2% bovine serum albumin) for 24 h at 4°C and then incubated with the iNOS or eNOS antibody (dilution, 1:100) at room temperature for 2 h, followed by washing three times with PBS. The blots were further incubated with the appropriate secondary antibodies conjugated to horseradish peroxidase (dilution, 1: 5,000). Following three washes with PBS, the immunoreactive bands were visualized by using enhanced chemiluminescence reagent (Pierce Co, Chicago, IL) and were exposed to X-ray film. The percent increase in iNOS or eNOS expression was calculated based on densitometry normalized to β-actin levels.

Flow cytometry

To detect the expression of iNOS or eNOS or GP96, HBMEC were infected with *E. coli* for various periods. After incubation, the cells were washed three times with PBS and then detached with 2.5 mM EDTA from the plates. The cells were first pre-incubated for 30 minutes with IgG blocking buffer to mask non-specific binding sites and then fixed and permeabilized using BD cytofix and cytoperm kit. Cells were then incubated with iNOS, eNOS, GP 96 or an isotype control antibody for 30 min at 4°C and then washed with BD permwash buffer. Then FITC conjugated secondary antibody was added, incubated for 20 min at 4°C, and washed with permwash buffer. The stained cells were then analyzed by four-color flow cytometry using FACS calibur Cell Quest Pro software (BD Biosciences, San Diego, CA) and at least 10,000 events were collected for analysis. Results are expressed as mean fluorescence intensity (MFI) subtracted from isotype matched control.

Immunofluorescence

HBMEC infected with either $OmpA^+$ or $OmpA^-$ *E. coli* were washed with RPMI 1640 and fixed with 2% paraformaldehyde in PBS for 15 min at room temperature. In some experiments, the inhibitors of iNOS or cGMP were incubated with HBMEC 1 h prior to addition of the bacteria. The cells were washed and permeabilized with 0.1% Triton X-100 in PBS containing 5% normal goat serum for 30 min at room temperature. Then the cells were incubated with anti-VE-cadherin antibodies (1: 1000 dilution) for 1 h, washed and further incubated with Cy3 coupled secondary antibodies (1: 2000 dilution). Finally the slides were washed and mounted

with Vectashield containing DAPI (Vector Laboratories, Burlingame, CA). Cells were viewed with a Leica (Wetzlar, Germany) DMRA microscope with Plan-apochromat ×40/1.25 NA and ×63/1.40 NA oil immersion objective lenses. Image acquisition was with a SkyVision-2/VDS digital CCD (12-bit, 1280 × 1024 pixel) camera in unbinned or 2 × 2-binned models into EasyFISH software, saved as 16-bit monochrome, and merged as 24-bit RGB TIFF images (Applied Spectral Imaging Inc., Carlsbad, CA). The images were processed by using Adobe Photoshop 7.0.

Transendothelial permeability assay

The passage of horseradish peroxidase (HRP) through confluent HBMEC monolayers was measured with transwell cell culture chambers (polycarbonate filters, 4.0-μm pore size; Costar, NY). HBMEC were seeded onto filter inserts in 200 μL of RPMI 1640 medium, as described for HBMEC culture. The lower compartment was filled with the same medium (600 μL). HBMEC were grown for 3–4 days to attain confluence. At the beginning of the experiment, the medium in the upper compartment was carefully removed and replaced with 200 μL of fresh medium or medium containing bacteria with or without pretreatment with NO inhibitors (4 μM) along with 0.1 μg of HRP. At this point, the lower compartment was also refilled with fresh medium. At several time points, 5-μL samples were withdrawn from the lower compartment. The HRP concentration was determined spectrophotometrically at 470 nm by measuring the peroxidase activity with 5 mmol/L guaiacol in 50 mmol/L $Na_2H_2PO_4$ in the presence of 0.7 mmol/L hydrogen peroxide. In addition, at every time point, TEER was measured with a Millipore ERS apparatus, according to manufacturer's protocol.

PepTag assay for non-radioactive detection of PKC activity—The PepTag (Promega) assay utilizes a florescent peptide substrate that is highly specific to PKC according to the manufacturer's instructions. Phosphorylation by PKC changes the net charge of the peptide substrate from +1 to −1, thereby allowing the phosphorylated and non-phosphorylated versions of the substrate to be separated using agarose (0.8%) gel electrophoresis. The phosphorylated species migrates toward the positive electrode, while the non-phosphorylated substrate migrates toward the negative electrode. HBMEC total lysates or membrane proteins (10–25 μg in 10 μl) were incubated with the PKC reaction mixture (25 μl) according to the manufacturer's protocol at 30 °C for 30 min. The reactions were stopped by placing the tubes in a boiling water bath. After adding 80% glycerol (1 μl), the samples were loaded onto an agarose gel (0.8% agarose in 50 mM Tris-HCl, pH 8.0) and separated at 100 V for 15 min. The peptide bands were visualized under UV light.

Estimation of NO production

To determine the production of NO by HBMEC following interaction with bacteria, $OmpA^+$ and $OmpA^-$ *E. coli* were added to the wells and incubated for varying periods. At completion of the experiment, supernatants were collected and analyzed for NO production by modified Greiss method as described earlier (Mittal *et al.*, 2008). Briefly nitrate was converted to nitrites with β-nicotinamide adenine dinucleotide phosphate (NADPH) (1.25 mg/ml) and nitrate reductase followed by addition of Griess reagent. The reaction mixture was incubated at room temperature for 20 min followed by addition of TCA. Samples were centrifuged, clear supernatants were collected, and optical density was recorded at 550 nm. The amounts of NO produced were determined by calibrating standard curve using sodium nitrite.

RT-PCR—HBMEC were grown to 90% confluence in 100 mm dishes and infected with *E. coli* for different periods. The cells were then washed, total RNA was extracted using RNAeasy kit (Qiagen, Valencia, CA) and RNA was quantified using the nanodrop machine. RT-PCR for iNOS and eNOS was performed using the following primer sequence: 5’ (sense) 5’-GCCTCGCTCTGGAAAGA-3’; 3’ (antisense) 5’-TCCATGCAGACAACCTT-3’ and

5’ (sense) 5’-CAGTGTCCAACATG CTGCTGGAAATTG-3’; 3’(antisense) 5’-TAAAGGTCTTCTTC CTG GTGATGCC-3’, respectively. GAPDH former and reverse primer sequences were TTGCCATCAATGACCCCTTCA and CGCCCCACTTGATTTTGGA, respectively.

siRNA transfection—HBMEC were grown to 30% confluence in 6-well plates, then transfected with siRNA for iNOS or eNOS or gp96 using Deliver X plus siRNA transfection kit (Panomics, Fremont, CA), according to manufacturer’s instructions. Deliver × plus provided >90% transfection efficiency while maintaining the cell viability. The siRNA primer sequence used for silencing iNOS transfection was CCACCAGTATGCAATGAAT (Invitrogen, Carlsbad, CA). The siRNA for silencing eNOS was purchased from Invitrogen (Carlsbad, CA) having oligo identification numbers HSS 107326, HSS 107327 and HSS 107328. The siRNA primer sequence for silencing gp96 was also purchased from Invitrogen (Carlsbad, CA) having oligo identification number HSS110955. The respective control siRNA were also purchased from Invitrogen (Carlsbad, CA).

cGMP estimation—The levels of cGMP were determined using a kit from Cayman chemicals (Ann Arbor, Michigan) according to manufacturer’s instructions.

Statistical Significance—Results were statistically analyzed using Student’s *t* test, ANOVA and Fisher two tailed test and $P<0.05$ was considered statistically significant.

Acknowledgments

We thank Catherine J. Hunter for critical reading of this manuscript. This work was supported by grants from NIH (AI40567 to N. V. P).

REFERENCES

Antonova G, Lichtenbeld H, Xia T, Chatterjee A, Dimitropoulou C, Catravas JD. Functional significance of hsp90 complexes with NOS and sGC in endothelial cells. Clin Hemorheol Microcirc 2007;37:19–35. [PubMed: 17641392]

Bogdan C. Nitric oxide and the immune response. Nat Immunol 2001;2:907–916. [PubMed: 11577346]

Boje KM. Inhibition of nitric oxide synthase attenuates blood-brain barrier disruption during experimental meningitis. Brain Res 1996;720:75–83. [PubMed: 8782899]

Boveri M, Kinsner A, Berezowski V, Lenfant AM, Draing C, Cecchelli R, et al. Highly purified lipoteichoic acid from gram-positive bacteria induces *in vitro* blood-brain barrier disruption through glia activation: role of pro-inflammatory cytokines and nitric oxide. Neuroscience 2006;137:1193–1209. [PubMed: 16343789]

Bratasz A, Kuter I, Konior R, Goscinski I, Lukiewicz S. Nitric oxide as a prognostic marker for neurological diseases. Antioxid Redox Signal 2004;6:613–617. [PubMed: 15130288]

Burgner D, Rockett K, Kwiatkowski D. Nitric oxide and infectious diseases. Arch Dis Child 1999;81:185–188. [PubMed: 10490536]

Cary SP, Winger JA, Derbyshire ER, Marletta MA. Nitric oxide signaling: no longer simply on or off. Trends Biochem Sci 2006;31:231–239. [PubMed: 16530415]

Chakravortty D, Hensel M. Inducible nitric oxide synthase and control of intracellular bacterial pathogens. Microbes Infect 2003;5:621–627. [PubMed: 12787738]

Chan ED, Chan J, Schluger NW. What is the role of nitric oxide in murine and human host defense against tuberculosis? Current knowledge. Am J Respir Cell Mol Biol 2001;25:606–612. [PubMed: 11713103]

Constantin D, Cordenier A, Robinson K, Ala'Aldeen DAA, Murphy S. *Neisseria meningitidis*-induced death of cerebrovascular endothelium: mechanisms triggering transcriptional activation of inducible nitric oxide synthase. J Neurochem 2004;89:1166–1174. [PubMed: 15147509]

Coureuil M, Mikaty G, Miller F, Lécuyer H, Bernard C, Bourdoulous S, Duménil G, Mège RM, Weksler BB, Romero IA, Couraud PO, Nassif X. Meningococcal type IV pili recruit the polarity complex to cross the brain endothelium. Science 2009;325:83–87. [PubMed: 19520910]

Denninger JW, Marletta MA. Guanylate cyclase and the NO/cGMP signaling pathway. Biochim Biophys Acta 1999;1411:334–350. [PubMed: 10320667]

Derbyshire ER, Marletta MA. Biochemistry of soluble guanylate cyclase. Handb Exp Pharmacol 2009;121:17–31. [PubMed: 19089323]

Engelhardt B. Development of the blood-brain barrier. Cell Tissue Res 2003;314:119–129. [PubMed: 12955493]

Golombek DA, Agostino PV, Plano SA, Ferreyra GA. Signaling in the mammalian circadian clock: the NO/cGMP pathway. Neurochem Int 2004;45:929–936. [PubMed: 15312987]

Hattor Y, Kasai K, Akimoto K, Thiemermann C. Induction of NO synthesis by lipoteichoic acid from *Staphylococcus aureus* in J774 macrophages: involvement of a CD14-dependent pathway. Biochem Biophys Res Commun 1997;233:375–379. [PubMed: 9144542]

Hoffmann O, Zweigner J, Smith SH, Freyer D, Mahrhofer C, Dagand E, et al. Interplay of Pneumococcal Hydrogen Peroxide and Host-Derived Nitric Oxide. Infect Immun 2006;74:5058–5066. [PubMed: 16926397]

Hou Y, Lascola J, Dulin NO, Ye RD, Browning DD. Activation of cGMP-dependent protein kinase by protein kinase C. J Biol Chem 2003;278:16706–16712. [PubMed: 12609995]

Jaworowicz DJ Jr, Korytko PJ, Singh LS, Boje KM. Nitric oxide and prostaglandin E2 formation parallels blood-brain barrier disruption in an experimental rat model of bacterial meningitis. Brain Res Bull 1998;46:541–546. [PubMed: 9744292]

Ji JY, Diamond SL. Exogenous nitric oxide activates the endothelial glucocorticoid receptor. Biochem Biophys Res Commun 2004;318:192–197. [PubMed: 15110772]

Khan SA, Strijbos PJ, Everest P, Moss D, Stratford R, Mastroeni P, et al. Early responses to *Salmonella typhimurium* infection in mice occur at focal lesions in infected organs. Microb Pathog 2001;30:29–38. [PubMed: 11162183]

Kim BY, Kang J, Kim KS. Invasion processes of pathogenic *Escherichia coli*. Int J Med Microbiol 2005;295:463–470. [PubMed: 16238020]

Kim KS. Strategy of *Escherichia coli* for crossing the blood-brain barrier. J Infect Dis 2002;186:S220–S224. [PubMed: 12424701]

Kim KS. Pathogenesis of bacterial meningitis: from bacteremia to neuronal injury. Nat Rev Neurosci 2003;4:376–385. [PubMed: 12728265]

Krumenacker JS, Murad F. NO-cGMP signaling in development and stem cells. Mol Genet Metab 2006;87:311–314. [PubMed: 16356747]

Lahiri A, Das P, Chakravortty D. Arginase modulates *Salmonella* induced nitric oxide production in RAW264.7 macrophages and is required for *Salmonella* pathogenesis in mice model of infection. Microbes Infect 2008;10:1166–1174. [PubMed: 18625332]

Leib SL, Tauber MG. Pathogenesis of bacterial meningitis. Infect Dis Clin North Am 1999;13:527–548. [PubMed: 10470554]

Maruvada R, Argon Y, Prasadarao NV. *Escherichia coli* interaction with human brain microvascular endothelial cells induces signal transducer and activator of transcription 3 association with the C-terminal domain of Ec-gp96, the outer membrane protein A receptor for invasion. Cell Microbiol 2008a;10:2326–2338. [PubMed: 18662321]

Maruvada R, Blom AM, Prasadarao NV. Effects of complement regulators bound to *Escherichia coli* K1 and Group B *Streptococcus* on the interaction with host cells. Immunology 2008b;124:265–276. [PubMed: 18028369]

Mayhan WG. Nitric oxide donor-induced increase in permeability of the blood-brain barrier. Brain Res 2000;866:101–108. [PubMed: 10825485]

Mittal R, Sharma S, Chhibber S, Harjai K. Contribution of free radicals to *Pseudomonas aeruginosa* induced acute pyelonephritis. Microb Pathog 2008;45:323–330. [PubMed: 18771720]

Murawska-Ciałowicz E, Szychowska Z, Trbusiewicz B. Nitric oxide production during bacterial and viral meningitis in children. Int J Clin Lab Res 2000;30:127–131. [PubMed: 11196070]

Murphy BA, Fakira KA, Song Z, Beuve A, Routh VH. AMP-activated Protein Kinase (AMPK) and Nitric Oxide (NO) regulate the glucose sensitivity of ventromedial hypothalamic (VMH) glucose-inhibited (GI) neurons. Am J Physiol Cell Physiol. 2009 (in press).

Nathan C, Xie QW. Nitric oxide synthases: roles, tolls, and controls. Cell 1994;78:915–918. [PubMed: 7522969]

Panjwani NN, Popova L, Srivastava PK. Heat shock proteins gp96 and hsp70 activate the release of nitric oxide by APCs. J Immunol 2002;168:2997–3003. [PubMed: 11884472]

Papapetropoulos A, Zhou Z, Gerassimou C, Yetik G, Venema RC, Roussos C, et al. Interaction between the 90-kDa heat shock protein and soluble guanylyl cyclase: physiological significance and mapping of the domains mediating binding. Mol Pharmacol 2005;68:1133–1141. [PubMed: 16024662]

Pearce WJ, Williams JM, White CR, Lincoln TM. Effects of chronic hypoxia on soluble guanylate cyclase activity in fetal and adult ovine cerebral arteries. J Appl Physiol 2009;107:192–199. [PubMed: 19407253]

Petrov AM, Giniatullin AR, Sitdikova GF, Zefirov AL. The role of cGMP-dependent signaling pathway in synaptic vesicle cycle at the frog motor nerve terminals. J Neurosci 2008;28:13216–13222. [PubMed: 19052213]

Polin RA, Harris MC. Neonatal bacterial meningitis. Semin Neonatol 2001;6:157–172. [PubMed: 11483021]

Poulos TL. Soluble guanylate cyclase. Curr Opin Struct Biol 2006;16:736–743. [PubMed: 17015012]

Prasadarao NV. Identification of *Escherichia coli* outer membrane protein A receptor on human brain microvascular endothelial cells. Infect Immun 2002;70:4556–4563. [PubMed: 12117968]

Prasadarao NV, Srivastava PK, Rudrabhatla RS, Kim KS, Huang SH, Sukumaran SK. Cloning and expression of the *Escherichia coli* K1 outer membrane protein A receptor, a gp96 homologue. Infect Immun 2003;71:1680–1688. [PubMed: 12654781]

Prasadarao NV, Wass CA, Weiser JN, Stins MF, Huang SH, Kim KS. Outer membrane protein A of *Escherichia coli* contributes to invasion of brain microvascular endothelial cells. Infect Immun 1996;64:146–153. [PubMed: 8557332]

Remer KA, Jungi TW, Fatzer R, Täuber MG, Leib SL. Nitric oxide is protective in listeric meningoencephalitis of rats. Infect Immun 2001;69:4086–4093. [PubMed: 11349080]

Selvaraj SK, Periandythevar P, Prasadarao NV. Outer membrane protein A of *Escherichia coli* K1 selectively enhances the expression of intercellular adhesion molecule-1 in brain microvascular endothelial cells. Microbes Infect 2007;9:547–557. [PubMed: 17368067]

Shin S, Lu G, Cai M, Kim KS. *Escherichia coli* outer membrane protein A adheres to human brain microvascular endothelial cells. Biochem Biophys Res Commun 2005;330:1199–1204. [PubMed: 15823570]

Stenger S, Donhauser N, Thuring H, Röllinghoff M, Bogdan C. Reactivation of latent leishmaniasis by inhibition of inducible nitric oxide synthase. J Exp Med 1996;183:1501–1514. [PubMed: 8666908]

Stins MF, Prasadarao NV, Ibric L, Wass CA, Luckett P, Kim KS. Binding characteristics of S fimbriated *Escherichia coli* to isolated brain microvascular endothelial cells. Am J Pathol 1994;145:1228–1236. [PubMed: 7977653]

Sukumaran SK, Prasadarao NV. Regulation of protein kinase C in *Escherichia coli* K1 invasion of human brain microvascular endothelial cells. J Biol Chem 2002;277:12253–12262. [PubMed: 11805101]

Sukumaran SK, Prasadarao NV. *Escherichia coli* K1 invasion increases human brain microvascular endothelial cell monolayer permeability by disassembling vascular-endothelial cadherins at tight junctions. J Infect Dis 2003;188:1295–1309. [PubMed: 14593586]

Sukumaran SK, McNamara G, Prasadarao NV. *Escherichia coli* K1 interaction with human brain microvascular endothelial cells triggers phospholipase C-gamma1 activation downstream of phosphatidylinositol 3-kinase. J Biol Chem 2003;278:45753–45762. [PubMed: 12952950]

Sukumaran SK, Quon MJ, Prasadarao NV. *Escherichia coli* K1 internalization via caveolae requires caveolin-1 and protein kinase C alpha interaction in human brain microvascular endothelial cells. J Biol Chem 2002;277:50716–50724. [PubMed: 12386163]

Suzuki Y, Fujii S, Tominaga T, Yoshimoto T, Fujii S, Akaike T, et al. Direct evidence of *in vivo* nitric oxide production and inducible nitric oxide synthase mRNA expression in the brain of living rat

during experimental meningitis. J Cereb Blood Flow Metab 1999;19:1175–1178. [PubMed: 10566963]

Tunbridge AJ, Stevanin TM, Lee M, Marriott HM, Moir JWB, Read RC, Dockrell DH. Inhibition of macrophage apoptosis by *Neisseria meningitidis* requires nitric oxide detoxification mechanisms. Infect Immun 2006;74:729–733. [PubMed: 16369030]

Tunkel AR, Scheld WM. Pathogenesis and pathophysiology of bacterial meningitis. Clin Microbiol Rev 1993;6:118–136. [PubMed: 8472245]

Venema RC, Venema VJ, Ju H, Harris MB, Snead C, Jilling T, et al. Novel complexes of guanylate cyclase with heat shock protein 90 and nitric oxide synthase. Am J Physiol Heart Circ Physiol 2003;285:H669–H678. [PubMed: 12676772]

Winter S, Konter J, Scheler S, Lehmann J, Fahr A. Permeability changes in response to NONOate and NONOate prodrug derived nitric oxide in a blood-brain barrier model formed by primary porcine endothelial cells. Nitric Oxide 2008;18:229–239. [PubMed: 18284923]

Wong D, Dorovini-Zis K, Vincent SR. Cytokines, nitric oxide, and cGMP modulate the permeability of an *in vitro* model of the human blood-brain barrier. Exp Neurol 2004;190:446–455. [PubMed: 15530883]

Woods ME, Olano JP. Host defenses to *Rickettsia rickettsii* infection contribute to increased microvascular permeability in human cerebral endothelial cells. J Clin Immunol 2008;28:174–185. [PubMed: 17957455]

Xie QW, Cho HJ, Calaycay J, Mumford RA, Swiderek KM, Lee TD, et al. Cloning and characterization of inducible nitric oxide synthase from mouse macrophages. Science 1992;256:225–228. [PubMed: 1373522]

Xie Y, Kim KJ, Kim KS. Current concepts on *Escherichia coli* K1 translocation of the blood-brain barrier. FEMS Immunol Med Microbiol 2004;42:271–279. [PubMed: 15477040]

Yoshida M, Xia Y. Heat shock protein 90 as an endogenous protein enhancer of inducible nitric-oxide synthase. J Biol Chem 2003;278:36953–36958. [PubMed: 12855682]

Zlokovic BV. The blood-brain barrier in health and chronic neurodegenerative disorders. Neuron 2008;57:178–201. [PubMed: 18215617]

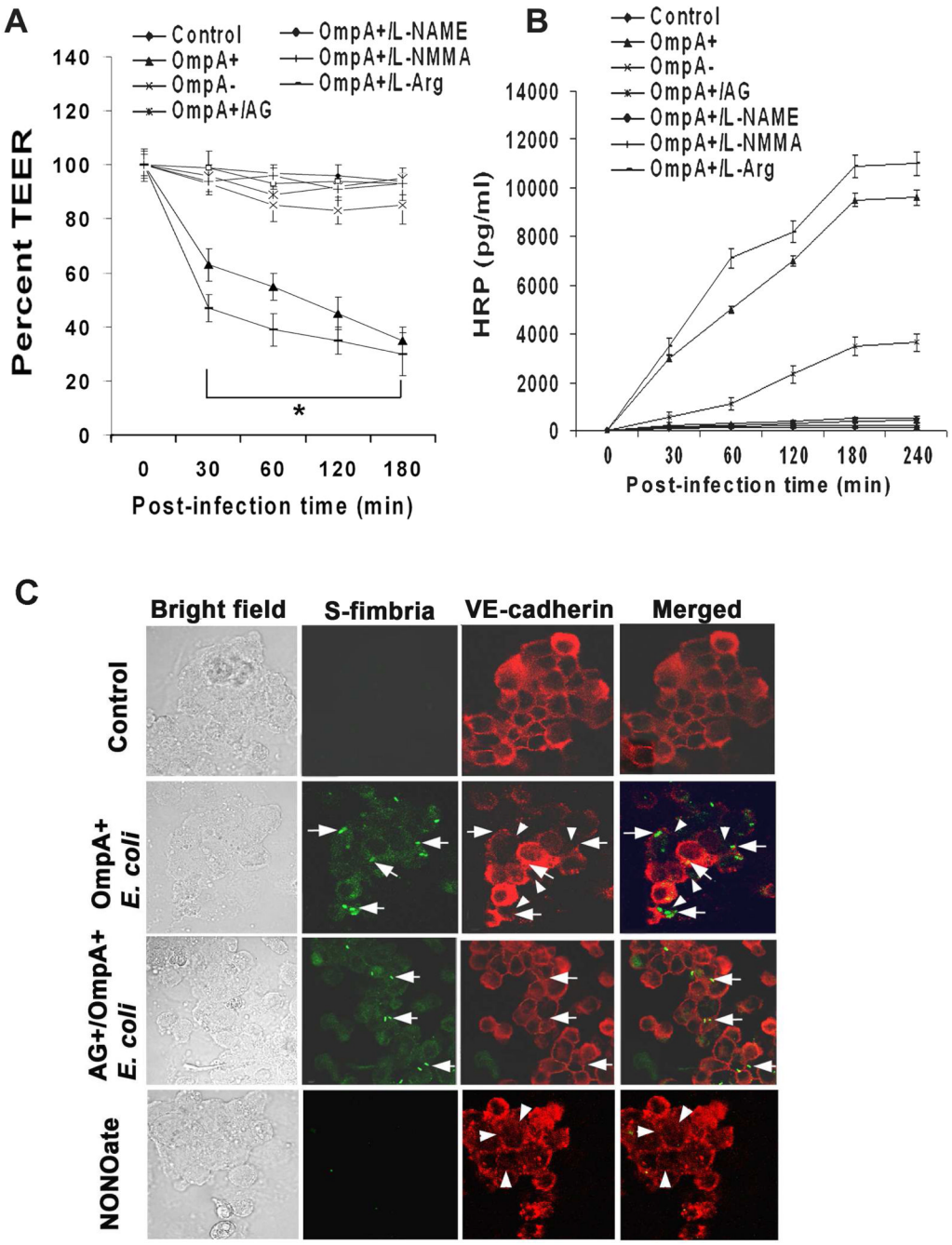

Fig. 1. Effects of NOS inhibitors on OmpA$^+$ *E. coli* induced permeability of HBMEC monolayers

Confluent monolayers of HBMEC grown in Transwell inserts were left untreated (Control), pretreated with NOS inhibitors (L-NAME, L-NMMA, or AG) and infected with OmpA$^+$ *E. coli* or OmpA$^-$ *E. coli* for indicated periods. L-Arginine (L-Arg) was used as a control. TEER (A) and HRP permeability (B) of the monolayers was measured as described in methods section. The experiments were performed at least three times in triplicate and the measurements are means ± SD. The decrease in TEER in HBMEC infected with OmpA$^+$ *E. coli* or OmpA$^+$ *E. coli*+L-arginine was significantly lower in comparison to control or OmpA$^-$ *E. coli* infected cells, $P<0.001$ by Student's *t* test. (C) Confluent monolayers of HBMEC in 8 well chamber slides were either uninfected or infected with OmpA$^+$ *E. coli* for 30 min without or pretreated

with AG and subjected to immunocytochemistry. In separate experiments, HBMEC were also treated with NONOate alone. The cells were washed, fixed, permeabilized and stained with anti-VE-cadherin antibodies followed by Cy3 conjugated secondary antibodies. The bacteria were stained with anti-S-fimbria antibody followed by FITC conjugated secondary antibody. The arrows indicate the position of the bacteria and the arrowheads indicate the disassembly of tight junctions. Original magnification × 40.

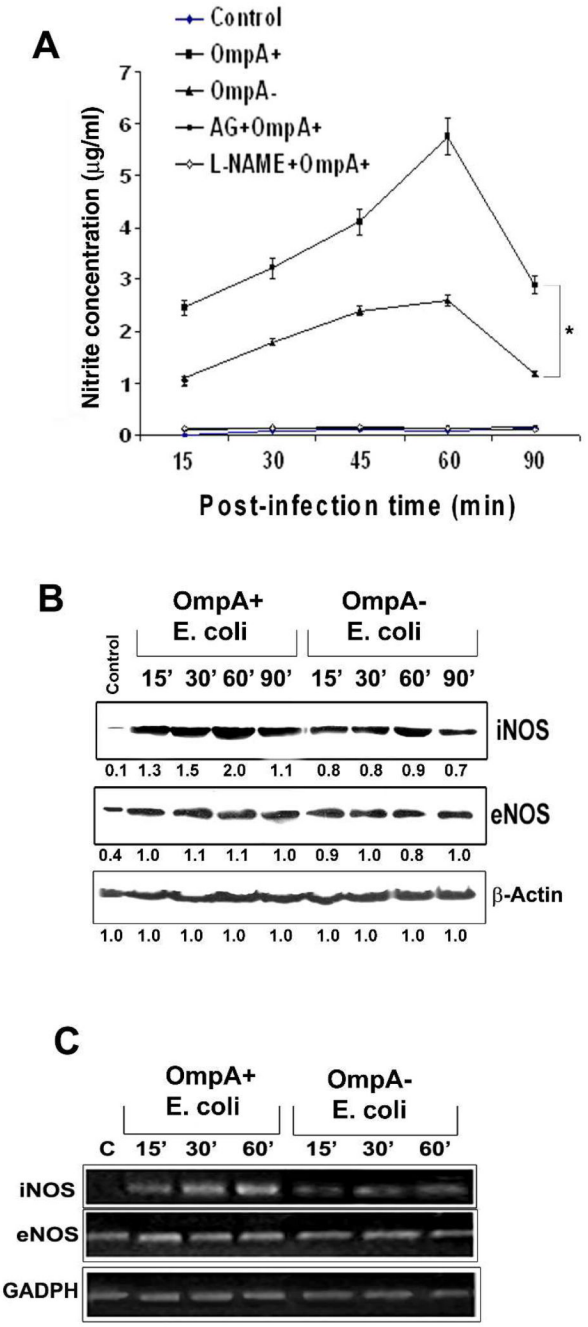

Fig. 2. OmpA$^+$ *E. coli* induces NO production by increasing the expression of iNOS in HBMEC

(A) Confluent monolayers of HBMEC in 24-well culture plates were treated with OmpA$^+$ or OmpA$^-$ *E. coli* for varying periods as indicated. Some monolayers were treated with AG or L-NAME for 1 h prior to addition of the bacteria. NO production in terms of nitrite was determined by Greiss method. (B) HBMEC monolayers infected with OmpA$^+$ or OmpA$^-$ *E. coli* were washed, total cell lysates prepared, and subjected to Western blotting with antibodies to iNOS, eNOS or β-actin. Total cell lysates from uninfected monolayers were used as control. The numbers indicate fold increase in intensities of the bands compared to control and were normalized to β-actin levels (C) Total RNA was isolated from the cells as treated in B and subjected to RT-PCR using primers for iNOS, eNOS, or GAPDH. These data in A represent

mean ± SD from three separate experiments performed in triplicate. The production of NO by $OmpA^+$ *E. coli* was significantly greater in comparison to the levels induced by $OmpA^-$ *E. coli* at all time points, **P*<0.001 by Student's *t* test.

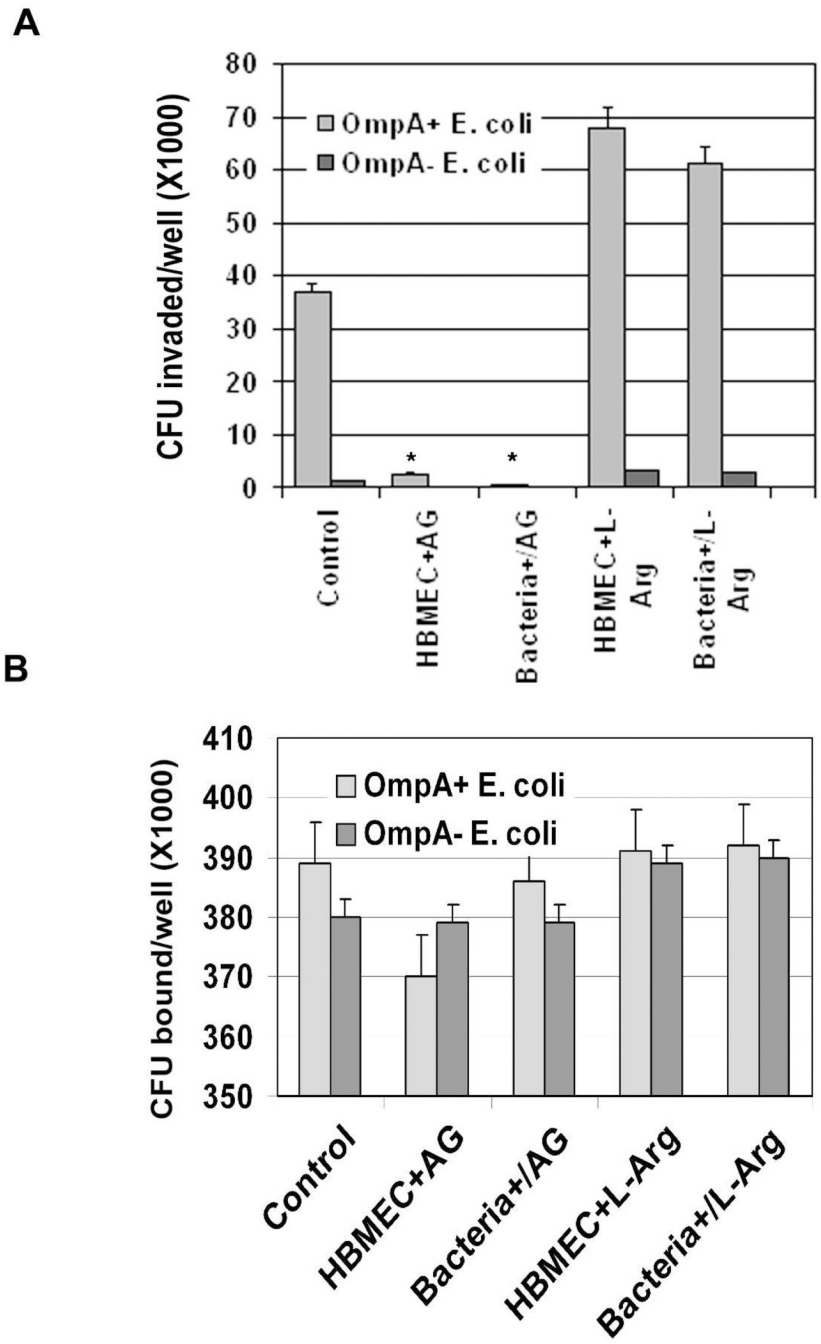

Fig. 3. Effects of NOS inhibitors on *E. coli* binding to and invasion of HBMEC

iNOS inhibitor, AG (4 μM) or L-arginine was incubated with HBMEC monolayers prior to adding *E. coli* (HBMEC+AG) or added together along with the bacteria (Bacteria+AG). Intracellular (A) or total cell associated bacteria (B) were determined as described in the methods section. The data are shown as means CFU invaded or bound per well ± SD from four different experiments performed in triplicate. **P*<0.001 by Student's *t* test compared to control.

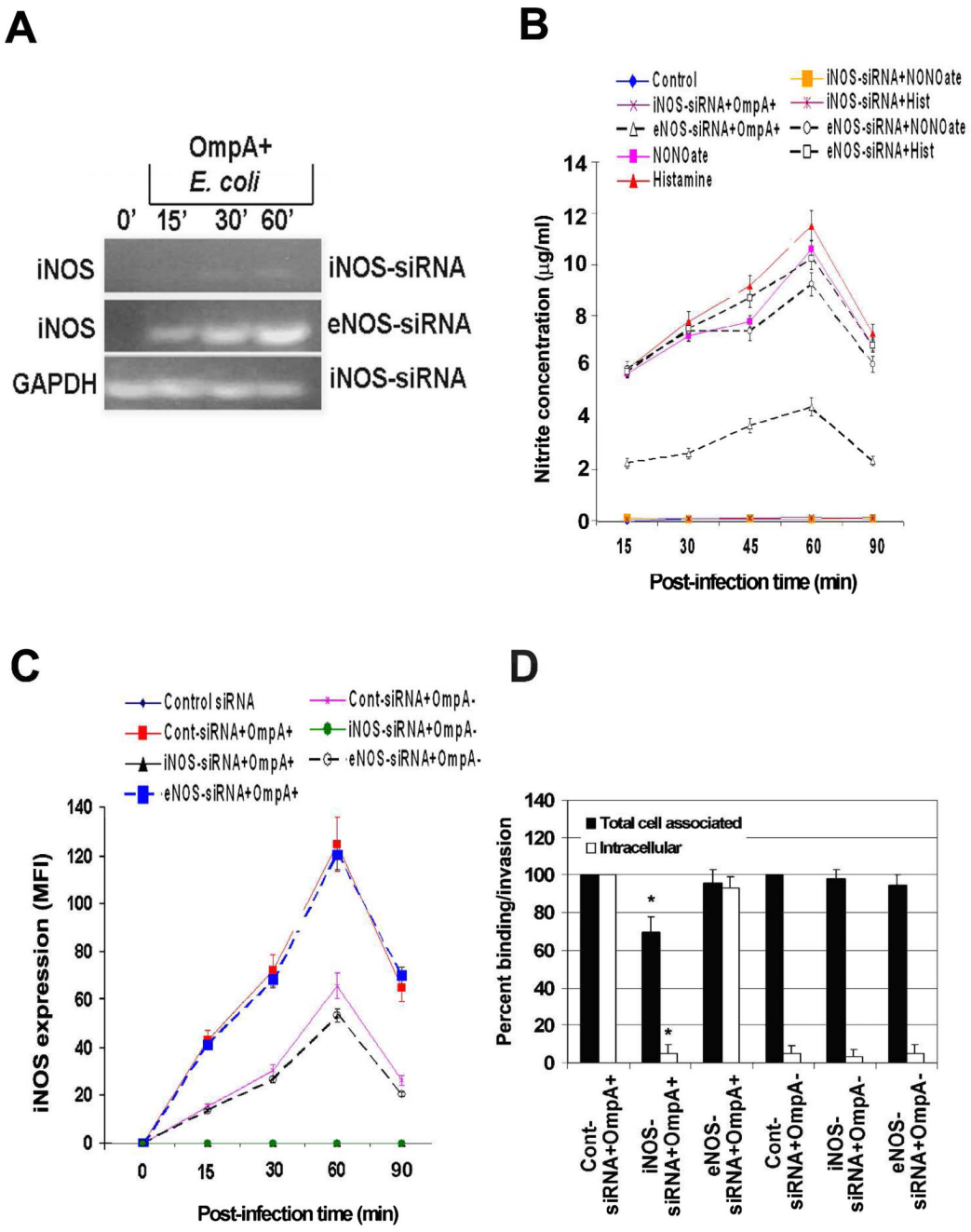

Fig. 4. Prevention of iNOS expression by siRNA inhibits OmpA$^+$ *E. coli* induced production of NO and thereby the invasion of the bacteria in HBMEC

(A) iNOS-siRNA/HBMEC or eNOS-siRNA/HBMEC transfected HBMEC were infected with OmpA$^+$ *E. coli* for indicated periods, total RNA was prepared, and subjected to RT-PCR using primers for iNOS or GAPDH. (B) HBMEC transfected with siRNA to iNOS or eNOS were incubated with OmpA$^+$ or OmpA$^-$ *E. coli* for varying periods, total cell lysates prepared, and NO production was determined by Greiss reagent. (C) In addition, the expression of iNOS in siRNA transfected HBMEC was also evaluated upon infection with OmpA$^+$ or OmpA$^-$ *E. coli* by flow cytometry. (D) The iNOS- or eNOS-siRNA transfected HBMEC were used for *E. coli* binding or invasion assays as described in the methods section (D). The data were

presented as percent binding (Total cell associated) or invasion (Intracellular) being taken the binding to or invasion of *E. coli* in control siRNA transfected HBMEC. The experiments were performed at least three times in triplicate. **P*<0.001 by Student's *t* test compared to control.

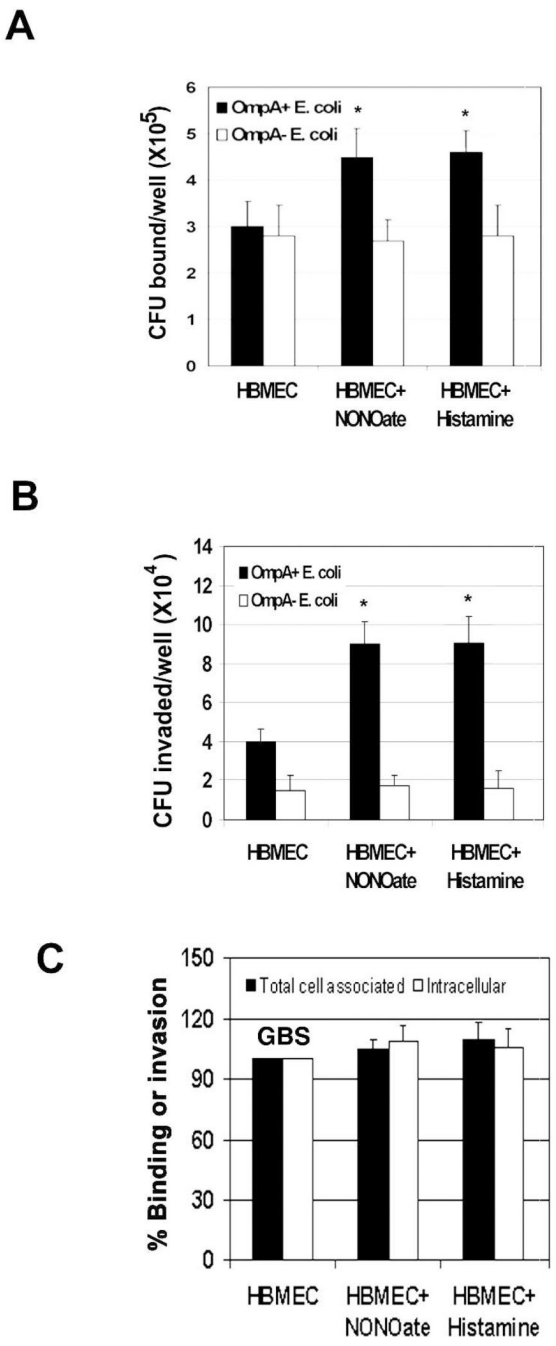

Fig. 5. The inducers of NO production increased the invasion of *E. coli* in HBMEC

Confluent monolayers of HBMEC were treated with NONOate or histamine for 1 h prior to the addition of *E. coli* (A and B) or GBS (C). Total bacteria bound to or invaded the monolayers was determined as described in the methods section. The data were presented as the number of CFU bound or invaded per well in case of *E. coli* or percent binding/invasion being taken the binding/invasion of GBS in control HBMEC as 100%. The experiments were performed at least three times in triplicate and the error bars represent SD. The increase in binding or invasion was significantly higher in NONOate or histamine treated HBMEC in comparison to control HBMEC (**P*<0.001 by Student's *t* test).

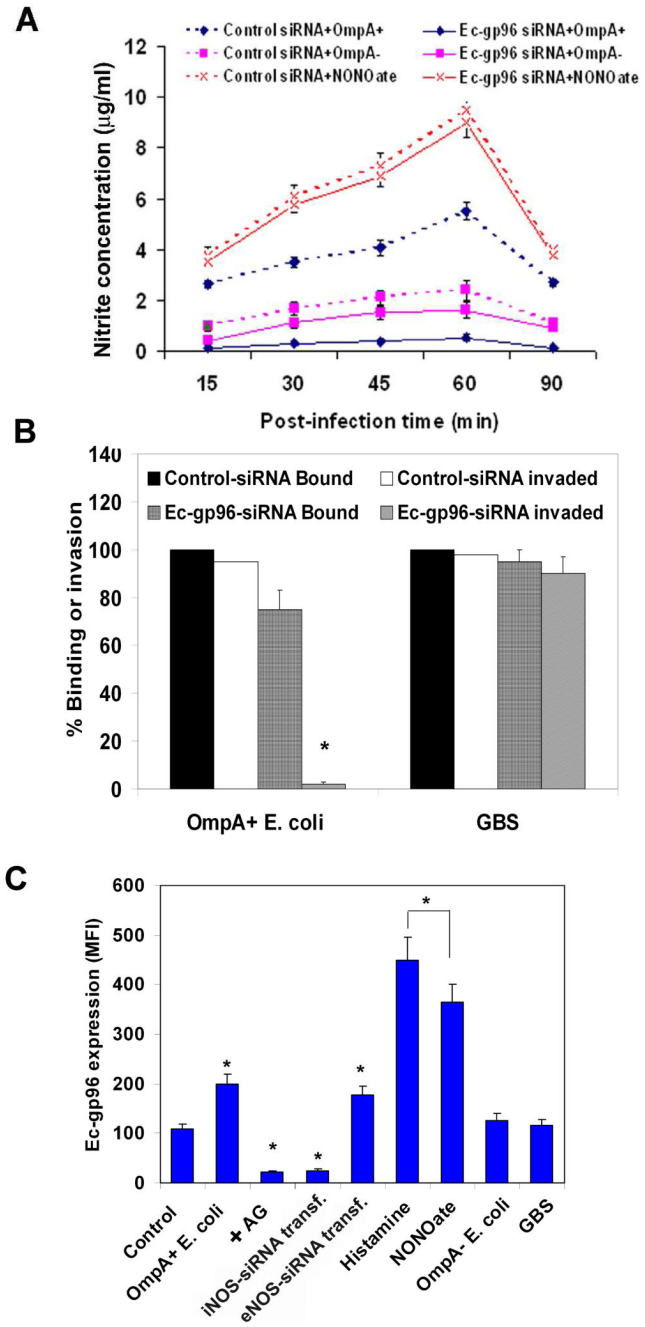

Fig. 6. Suppression of Ec-gp96 expression prevents *E. coli*–induced NO production in HBMEC

(A) HBMEC at 30% confluence were transfected with control-siRNA or Ec-gp96-siRNA and allowed to grow to confluence for three days. The cells were tested for the production of NO upon infection with $OmpA^+$ or $OmpA^-$ *E. coli* or treatment with NONOate. (B) Ec-gp96-siRNA/HBMEC or control-siRNA/HBMEC were subjected to binding and invasion assays with *E. coli* or GBS. The results are expressed as percent binding to or invasion being taken the binding/invasion in control cells as 100%. (C) HBMEC monolayers subjected to various treatments were analyzed for the expression of Ec-gp96 by flow cytometry as described in methods section. All experiments were performed at least three times in triplicate. The increase

or decrease in binding to or invasion and the expression of Ec-gp96 was significantly different in comparison to control, *P<0.001 by Student's t test.

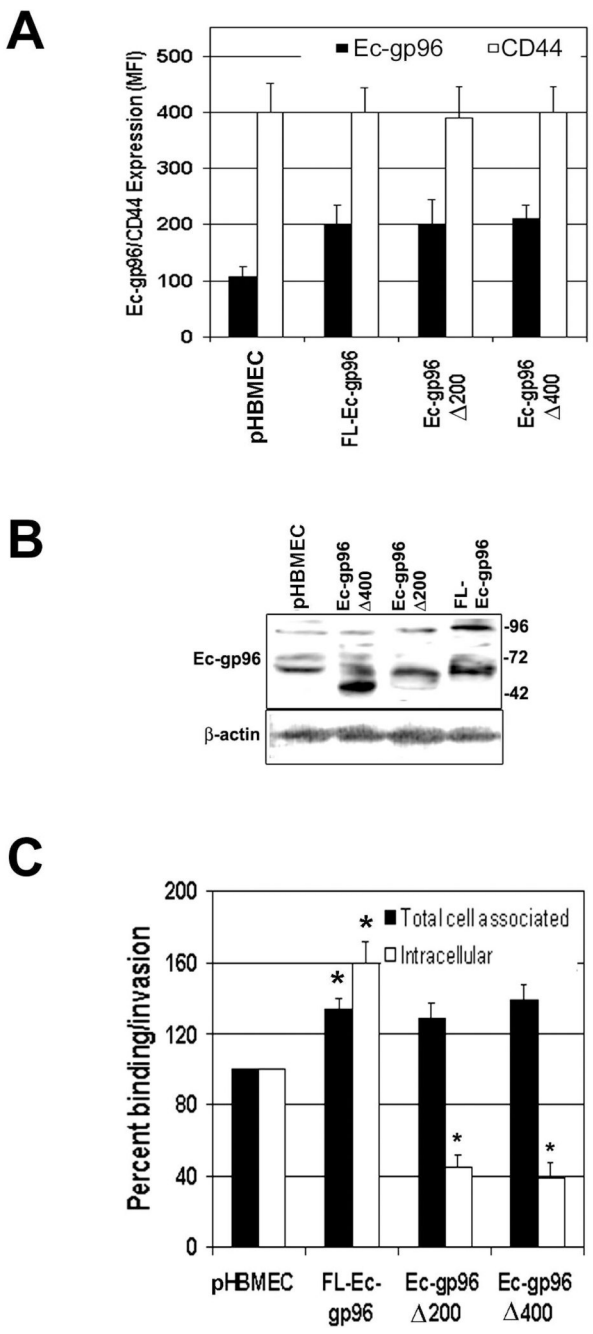

Fig. 7. Overexpression of C-terminal truncated Ec-gp96 proteins in HBMEC inhibits OmpA$^+$ *E. coli* invasion

HBMEC transfected with plasmid constructs containing C-terminal 200 (Ec-gp96Δ200) or 400 (Ec-gp96Δ400) amino acids deleted or full-length (FL-Ec-gp96) were subjected to flow cytometry to examine the expression of the truncated proteins or CD44, used as a control (A). Total cell lysates were also prepared from HBMEC transfectants and subjected to Western blotting with antibodies to Ec-gp96 or β-actin (B). The transfected HBMEC from A were used for *E. coli* binding and invasion experiments as described in the materials section and the data are expressed as percent values being taken the parameters of control HBMEC as 100% (C). The experiments were performed using cells from three different transfections. All values

represent means ± SD from four separate experiments performed in triplicate. The increase or decrease in binding or invasion was significant higher or lower in transfected HBMEC in comparison to plasmid alone transfected HBMEC, *P<0.001 by Student's t test.

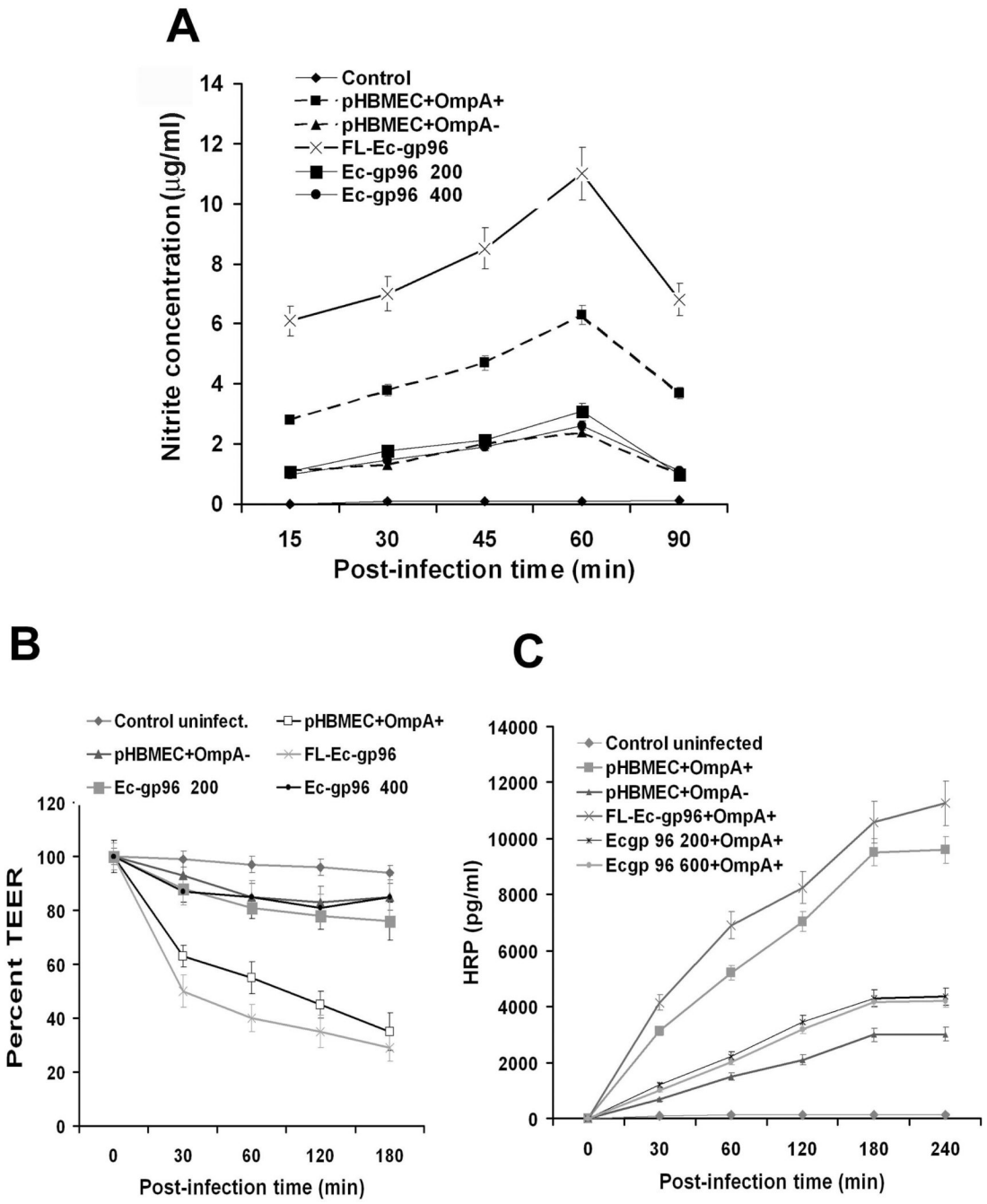

Fig. 8. Overexpression of C-terminal truncated Ec-gp96 proteins in HBMEC prevent the production of NO, decrease the TEER, and increase the permeability induced by OmpA$^+$ *E. coli*

HBMEC transfected with plasmid alone (pHBMEC) or plasmids containing C-terminal truncations of Ec-gp96 as described in Fig. 7 were infected with OmpA$^+$ *E. coli* for varying periods. The concentrations of NO in the supernatants were determined by Griess reagent (A). Both TEER (B) and HRP leakage (C) were assessed using the transfectant HBMEC monolayers after infecting with OmpA$^+$ *E. coli.* The experiments were performed three times in triplicate. The error bars represent SD.

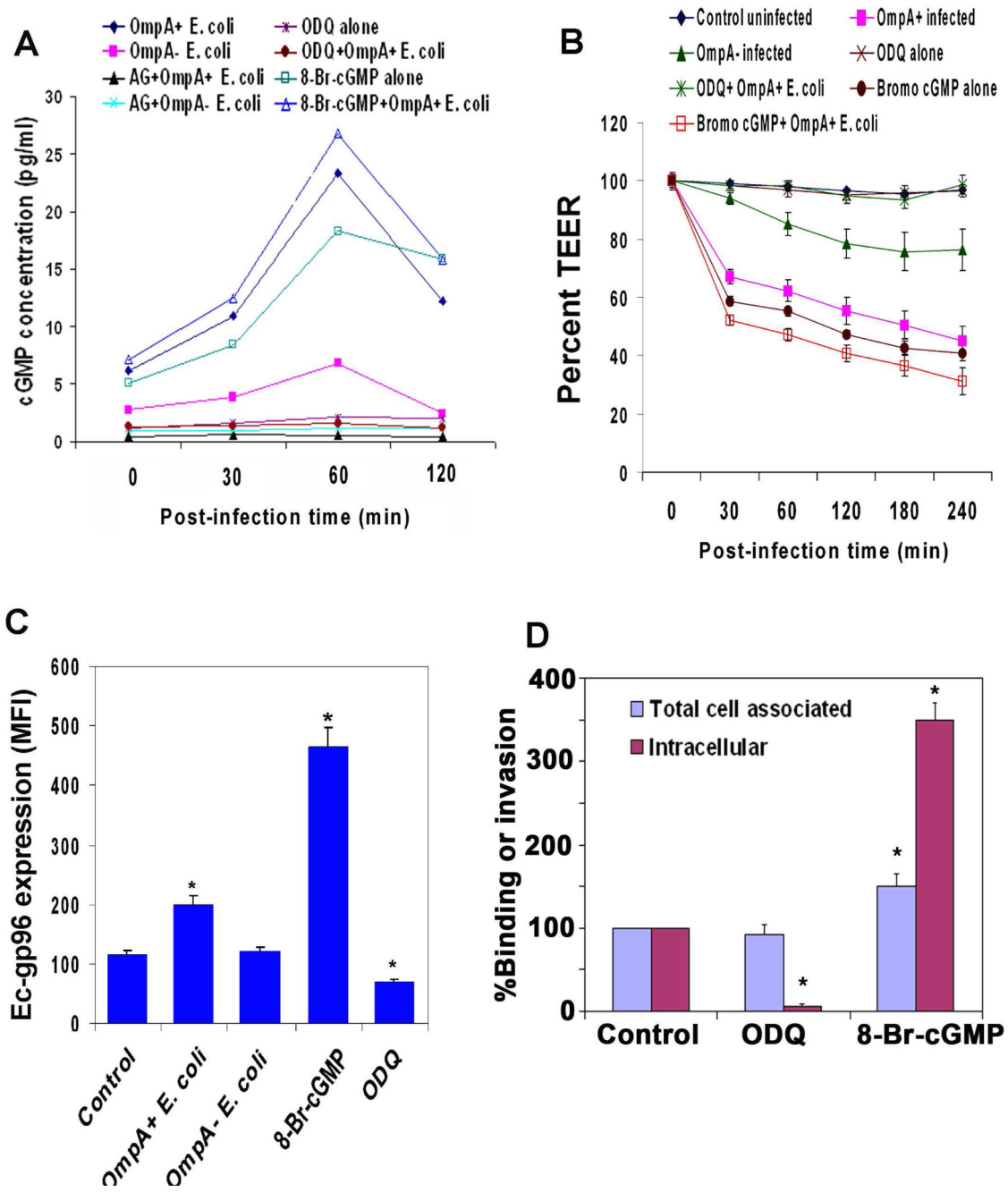

Fig. 9. OmpA$^+$ *E. coli* interaction with HBMEC induces NO mediated cGMP production, thereby enhancing the expression of Ec-gp96 for increased invasion

(A) Confluent monolayers of HBMEC were infected with OmpA$^+$ or OmpA$^-$ *E. coli* for varying periods, total cell lysates were prepared and the levels of cGMP were determined as described in the methods section. In some experiments, the monolayers were pretreated with AG, ODQ or 8-Br-cGMP prior to infection with the bacteria. (B) HBMEC were seeded onto Transwell filters and treated as described in A and the TEER was measured. (C) HBMEC were either untreated or infected with OmpA$^+$ or OmpA$^-$ *E. coli* or treated with 8-Br-cGMP or ODQ for 1 h. The cells were then subjected to flow cytometry analysis after staining with anti-Ec-gp96 antibodies. (D) HBMEC monolayers pretreated with ODQ or 8-Br-cGMP were subjected

to binding and invasion assays using $OmpA^+$ *E. coli*. The results are expressed as percent binding or invasion considering the binding/invasion of control HBMEC as 100%. All these experiments were performed at least three times in triplicates and presented as mean ± SD. The increase or decrease in the expression of Ec-gp96, binding to or invasion was significant compared to control HBMEC (**P*<0.001 by Student's *t* test).

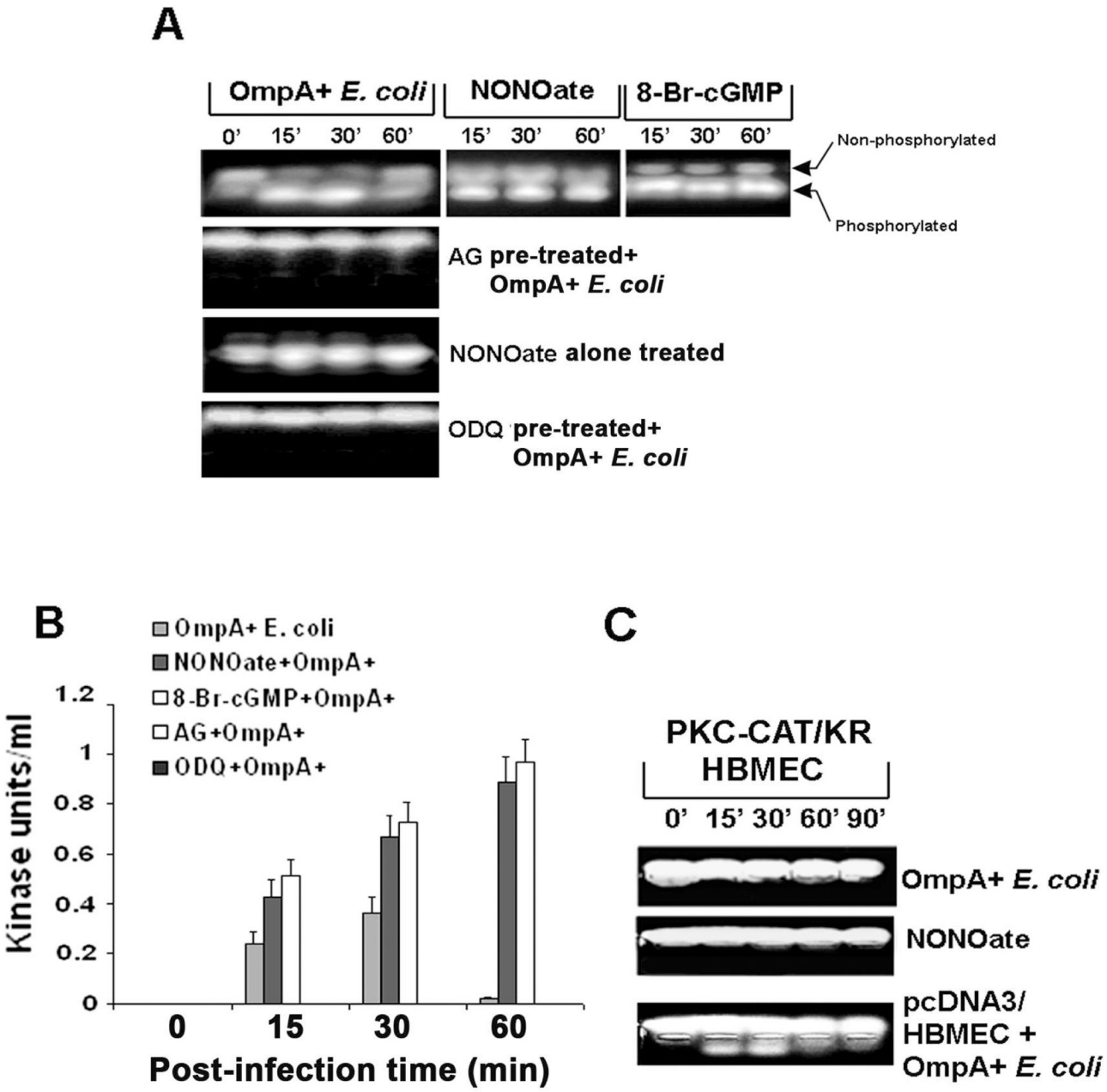

Fig. 10. Activation of PKC-α requires the production of cGMP in HBMEC upon infection with OmpA$^+$ *E. coli*

(A) HBMEC were infected with OmpA$^+$ *E. coli* after pre-treating the cells with AG, NONOate, or ODQ for 1 h as described in the methods section. In some experiments, HBMEC were treated with NONOate or 8-Br-cGMP alone for 1 h. The total cell lysates were subjected to non-radioactive PepTag assay to determine the PKC-α activity. (B) The phosophorylated peptide bands were excised and determined the concentration by a colorimetric assay as described in the methods section and expressed as kinase units/ml. (C) HBMEC were transfected with plasmid alone or a dominant negative form of PKC-α (PKC-CAT/KR), either untreated or treated with NONOate for 1 h, and infected with OmpA$^+$ *E. coli* for varying periods. The total

cell lysates were then subjected to PepTag assay. All experiments were performed at least three times. The error bars in panel B represent standard deviation from the means.

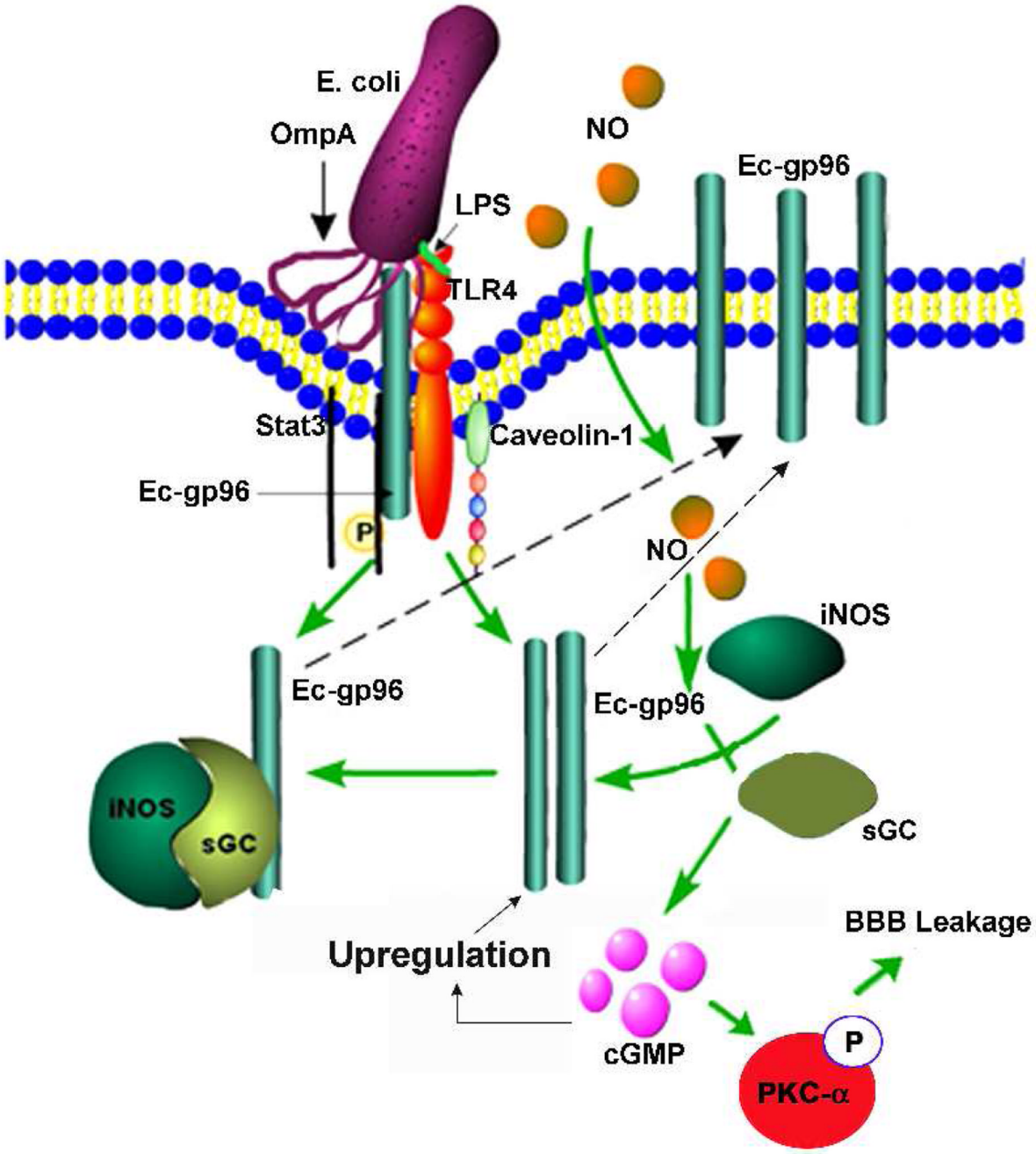

Fig. 11. Hypothetical mechanism of OmpA$^+$ *E. coli* induced expression of Ec-gp96 in HBMEC

OmpA initially interacts with constitutively expressed Ec-gp96 to activate iNOS, which in turn produces NO. Subsequently, NO enters HBMEC and further activates iNOS and soluble guanylyl cyclase (sGC), which together forms a complex. sGC induces cGMP production, which is responsible for the activation of PKC-α and thereby increased permeability of HBMEC monolayers. The formation of iNOS/sGC complexes requires Ec-gp96 in the cytosol. The recruitment of iNOS/sGC complex to the plasma membrane may drive Ec-gp96 also to the membrane. Additional Ec-gp96 molecules expressed at the plasma membrane becomes receptors to OmpA$^+$ *E. coli* to further invade HBMEC.